OULUN YLIOPISTO
UNIVERSITY of OULU
DEGREE PROGRAMME IN ELECTRICAL ENGINEERING

AVERAGE POWER TRACKING OPTIMIZATION SYSTEM FOR LTE POWER AMPLIFIERS

Thesis author _____
Ville Lehtisalo

Supervisor _____
Timo Rahkonen

Accepted _____/_____2014

Grade _____

Lehtisalo V. (2014) Average Power Tracking Optimization System for LTE Power Amplifiers. University of Oulu, Department of Electrical Engineering. Master's Thesis, 56 p.

ABSTRACT

This thesis introduces the design and implementation of an optimization system for average power tracking, used in the RF power amplifier of LTE mobile device. Average power tracking adjusts the supplied voltage of the power amplifier according to output power level so that the linearity of the power amplifier is maintained while the efficiency is improved. The optimization system is implemented with computer controlled measurement equipment setup. The setup consists of an RF signal generator, a power meter and a spectrum analyzer.

Performance measurements are performed to the device under test with different bias voltages of the PA and various output power levels, separately for two different power modes of the power amplifier. The performance measurements focus on the ratio of transmission channel power and adjacent channel power. Total efficiency and gain of the device and the current consumption of the power amplifier were also measured.

Based on the measurement results, the most suitable voltage for the power amplifier can be selected for each power level with a voltage table optimizing algorithm. The algorithm compares the measured adjacent channel leakage ratio to a predetermined target value and selects the lowest linearity requirements fulfilling a voltage value for the power amplifier. The effects of output power and supplied voltage on the linearity, gain and efficiency of the device are observed. The results show that the performance of the device under test is greatly dependent on the bias voltage of the power amplifier.

In addition, the effect of ambient temperature and different frequency channels on the linearity and gain are observed. The measurements show that the temperature affects marginally the gain whereas linearity is more dependent on the used frequency channel.

Finally the suitability of the optimized bias voltage table is verified by using it to adjust the power amplifier of a separate test board. The linearity of the product is verified by measuring the adjacent channel leakage ratio and comparing it to official requirements.

The voltage table generated with the optimizing algorithm based on the results obtained with the measurement setup is well suited for improving the power amplifier efficiency with average power tracking. It is a fast method to obtain a wide range of measurement results of the performance of a power amplifier with various output power levels and bias voltages.

Key words: average power tracking, LTE, power amplifier, linear performance

Lehtisalo V. (2014) Keskimääräisen tehonseurannan optimointisysteemi LTE-tehovahvistimille. Oulun yliopisto, sähkötekniikan osasto. Diplomityö, 56 s.

TIIVISTELMÄ

Tässä diplomityössä esitellään LTE-tiedonsiirtotekniikkaa tukevassa matkapuhelimessa käytettävän RF-tehovahvistimen keskimääräisen tehonseurannan optimointisysteemin suunnittelu ja toteutus. Keskimääräinen tehonseuranta säätää tehovahvistimen käyttöjännitettä lähtötehon perusteella niin, että tehovahvistimen lineaarisuus säilytetään ja hyötysuhde paranee. Optimointisysteemi toteutettiin tietokone-ohjatulla mittalaitekokoonpanolla sekä tulostenkäsittelyalgoritmilla. Mittalaitekokoonpano koostuu RF-signaaligeneraattorista, tehomittarista ja spektrianalysaattorista.

Testilaitteelle suoritetaan suorituskykymittauksia eri tehovahvistimen jännitearvoilla ja usealla lähtötehotasolla, erikseen kahdelle eri vahvistimen tehotilalle. Suorituskykymittaukset keskittyvät lähetyskanavan sekä viereisen kanavan tehon suhteen mittaukseen. Myös hyötysuhde, kokonaisvahvistus sekä testilaitteen tehovahvistimen virrankulutus mitataan suorituskykymittausten yhteydessä.

Mittaustulosten perusteella jännitetaulukon optimointialgoritmilla saadaan valittua sopivin tehovahvistimelle syötettävä jännite kullekin lähtötehotasolle. Algoritmi vertaa viereisen kanavan vuototehon suuruutta asetettuun tavoitearvoon ja valitsee tehovahvistimelle matalimman lineaarisuusvaatimukset täyttävän jännitteen. Havaintoja tehdään testilaitteen tehovahvistimen lineaarisuuden, vahvistuskertoimen ja hyötysuhteen riippuvuudesta lähtötehoon sekä käyttöjännitteeseen. Tuloksista nähdään syötettävän jännitteen vaikuttavan voimakkaasti testilaitteen suorituskykyyn.

Myös ympäröivän lämpötilan sekä taajuuskanavan vaikutusta tehovahvistimen lineaarisuuteen ja vahvistuskertoimeen tutkitaan. Mittaukset osoittavat lämpötilan vaikuttavan tehovahvistimen vahvistuskertoimeen marginaalisesti. Sen sijaan lineaarisuuteen vaikuttaa enemmän käytettävä taajuuskanava.

Lopuksi optimoidun jännitetaulukon soveltuvuus varmistetaan käyttämällä sitä erillisellä testilevyllä tehovahvistimen jännitteen säätämiseen. Varmistusmittauksissa lineaarisuus testataan mittaamalla viereisen kanavan vuototehon suuruus ja vertaamalla sitä asetettuihin virallisiin vaatimuksiin.

Mittalaitekokoonpanolla saatujen mittaustulosten sekä optimointialgoritmin perusteella luotu jännitetaulukko soveltuu hyvin tehovahvistimen hyötysuhteen parantamiseen keskimääräisen tehonseurannan avulla. Se on nopea tapa saada mittaustuloksia tehovahvistimen suorituskyvystä laajalta lähtötehoalueelta eri jännitearvoilla.

Avainsanat: keskimääräinen tehonseuranta, LTE, tehovahvistin, lineaarinen suorituskyky

TABLE OF CONTENTS

FOREWORD

This Master's Thesis was done for Microsoft Mobile Oy. The main purpose was to design and implement an RF power amplifier measurement setup and result processing algorithm for efficiency improvement. My supervisor at Microsoft Mobile was Lic.Sc. Samuli Pietilä and I would like to thank him for this opportunity. I am grateful to B.Sc. Janne Olli for his assistance with the setup, and M.Sc. Paavo Väänänen for answering my questions and guiding me through the measurement process. I also like to thank B.Sc. Jarno Luukkonen for providing the subject for this thesis, and M.Sc. Marjo Yli-Paavola and B.Sc. Gary Horning for helping with language revision. Big and warm compliments go to the whole RF team in Tampere for an inspiring and encouraging atmosphere. I sure had a great time working with you.

This thesis was supervised by Professor Timo Rahkonen and Ph.D. Janne Aikio. I would like to thank them for guidance and valuable feedback. Finally, I would like to thank my family and friends, especially my lovely girlfriend Anna-Sofia for her patience and support through the writing process.

Tampere, June 27th, 2014

Ville Lehtisalo

LIST OF ABBREVATIONS AND SYMBOLS

3GPP	3rd Generation Partnership Project
ACLR	Adjacent Channel Leakage Ratio
AM-AM	Amplitude-to-Amplitude distortion
AM-PM	Amplitude-to-Phase distortion
APT	Average Power Tracking
ASM	Antenna Switch Module
BOM	Bill of Material
BW	Bandwidth
CP	Cyclic Prefix
DC	Direct Current
DFT	Discrete Fourier Transform
DUT	Device Under Test
ET	Envelope Tracking
E-UTRA	Evolved Universal Terrestrial Radio Access
$E\text{-}UTRA_{ACLR}$	Adjacent channel leakage ratio with 3GPP E-UTRA limits
FE	Front-End
GPIO	General Purpose Input/Output
GSM	Global System for Mobile Communications
GMSK	Gaussian Minimum Shift Keying
HB	High frequency Band
HPM	High Power Mode of the Power Amplifier
HSPA	High-Speed Packet Access
IIP_3	Third Order Intercept Point Referred to the Input Power
IM	Intermodulation
IMD	Intermodulation Distortion
IP_3	Third Order Intercept Point
ISI	Inter-Symbol Interference
LB	Low frequency Band
LNA	Low Noise Amplifier
LPM	Low Power Mode of the Power Amplifier
LTE	Long Term Evolution
MIPI	Mobile Industry Processor Interface
MMMB	Multi-Mode Multiband
MPR	Maximum Power Reduction
NF	Noise Figure
OFDMA	Orthogonal Frequency-Division Multiple Access
OIP_3	Third Order Intercept Point Referred to the Output Power
OOB	Out-of-Band
P1dB	1 dB compression point
PA	Power Amplifier
PAE	Power Added Efficiency
PAM	Power Amplifier Module
PAPR	Peak-to-Average Power Ratio
PSU	Power Supply Unit
PWB	Printed Wired Board
QAM	Quadrature Amplitude Modulation
QPSK	Quadrature Phase Shift Keying

RB	Resource Block
RF	Radio Frequency
RFIC	Radio Frequency Integrated Circuit
RRC	Root-Raised-Cosine
RX	Receiver
SC-FDMA	Single-Carrier Frequency-Division Multiple Access
SEM	Spectrum Emission Mask
TX	Transmitter
UE	User Equipment
UMTS	Universal Mobile Telecommunications System
UTRA	Universal Terrestrial Radio Access
$UTRA_{ACLR1}$	First adjacent channel leakage ratio with 3GPP UTRA limits
$UTRA_{ACLR2}$	Second adjacent channel leakage ratio with 3GPP UTRA limits
VBA	Visual Basic for Applications
WCDMA	Wideband Code-Division Multiple Access

$ACLR_{MEAS}$	Measured adjacent channel leakage ratio
$ACLR_{TARG}$	Adjacent channel leakage ratio target
°C	Celsius degree
dB	Decibel
dBc	Decibels relative to carrier
dBm	Decibels relative to milliwatt
f_{ADJ}	Adjacent channel center frequency
f_0	Fundamental frequency
f_{IM}	Intermodulation frequency component
G	Gain of the power amplifier
G_{GUESS}	Gain guess of power amplifier gain
I_B	Base current
I_C	Collector current
I_{QC}	Quiescent current
kHz	Kilohertz
MHz	Megahertz
ms	Millisecond
N_{RB}	Transmission channel configuration
P_{AVG}	Average transmit power
P_{DC}	Direct current power
P_{IN}	RF input power
P_{IN_MAX}	Maximum input power from signal generator
P_{MAX}	Maximum output power
P_{OUT}	RF output power
P_{PEAK}	Peak transmit power
P_{STEP}	Output power step
P_{TARG}	Output power target
R_L	Load resistance
V_{BATT}	Battery voltage
V_{BIAS}	Bias voltage
V_{BIAS}	Power amplifier collector voltage
V_{CE}	Voltage between collector and emitter
V_{MAX}	Maximum bias voltage

v_o	Output voltage
$V_{O(dc)}$	DC-component of the output signal
v_s	Source voltage
V_{STEP}	Bias voltage step
α	Roll-off factor
Δf_{OOB}	Frequency from edge of channel bandwidth
θ	Conduction angle of the transistor

1. INTRODUCTION

The Radio Frequency (RF) Power Amplifiers (PA) in advanced systems like Long Term Evolution (LTE) [1] mobile devices should handle modulated signals with high Peak-to-Average Power Ratio (PAPR) while maintaining linearity and power efficiency. The PA is the most crucial component of the transmitter as its efficiency affects battery life and the output power and linearity correlate directly to the performance of the User Equipment (UE) [2].

Today's commercial PA is able to operate on multiple frequency bands and to have multimode capability. When operating at a low power region the efficiency of the PA is degraded significantly if current consumption is not optimized. Envelope Tracking (ET) [3] is very suitable, yet a quite newly realized solution for multimode operation and provides high efficiency. In terms of simplicity and low cost, Average Power Tracking (APT) is still very popular solution on the market for mobile handset efficiency improvement [4].

This thesis focuses on the efficiency improvement by optimizing the bias voltages of the PA with APT. It controls the supply voltage of the power amplifier according to the average power level at the 3rd Generation Partnership Project (3GPP) [5] specified transmission slot rate by utilizing a DC-DC converter.

The purpose of the measurement system is to measure the performance metrics of a Device Under Test (DUT), so that optimum bias voltages for the APT table can be generated. An optimized APT voltage table is generated with a dedicated measurement result processing algorithm. It takes the linear performance of the PA, measured with the Adjacent Channel Leakage Ratio (ACLR), into account while the efficiency is improved and 3GPP specified requirements are fulfilled. The generated APT table is then applied to a separate test board and linear performance of the device is verified by measurements.

This thesis consists of RF power amplifier theory in Chapter 2. The introduction and properties of LTE and specifications for user equipment transmission are presented in Chapter 3. The components used in the Front-End (FE) of a mobile device are introduced in Chapter 4. Chapter 5 describes the measurement setup and the device under test and the measurement results are presented and observed in Chapter 6. Chapter 7 discusses about possible future improvements of the system and Chapter 8 is the conclusion of this thesis.

2. POWER AMPLIFIER THEORY

This chapter introduces the PA operation classes used in radio frequency solutions and the main aspects in describing the performance of the PA. Also different techniques for efficiency improvement are proposed.

2.1. Performance Metrics

Power Added Efficiency

The efficiency of a basic amplifier is described simply by dividing output power with input power. With RF power amplifiers, where the input power is also substantial, Power Added Efficiency (PAE) is more commonly used figure of merit. It takes RF input power into account and gives eventually more precise concept of efficiency. Power added efficiency is defined with the equation

$$PAE = \frac{P_{\mathrm{OUT}} - P_{\mathrm{IN}}}{P_{\mathrm{DC}}}, \tag{1}$$

where P_{OUT} is RF output power and P_{IN} is RF input power of the PA. P_{DC} is DC power delivered to the PA. Power that is not converted to RF power is dissipated as heat. At high output power level minor losses in components and circuit can reduce total PAE by 10-15 %. [6]

Peak-to-Average Power Ratio

Peak-to-average power ratio is defined as the ratio of the maximum power and the average power value of the transmitted signal. It illustrates how much the output power varies between the maximum and average power level. It is described by

$$PAPR = \frac{P_{\mathrm{PEAK}}}{P_{\mathrm{AVG}}}, \tag{2}$$

where P_{PEAK} is the peak power and P_{AVG} is the average power of the signal. PAPR is used to express the variation of the signal envelope, typically in decibels. More complex modulation schemes including multicarrier transmission tend to have higher PAPR due to a large amplitude envelope variation in time domain. Peak and average signal powers and how they correlate with signal is demonstrated in Figure 1. [2]

1 dB Compression Point

The point, where the input signal level is increased to the point where the output signal is compressed 1 dB from the extrapolated linear gain, is called the 1 dB Compression Point (P1dB). This parameter is commonly used as a measure of linearity of power amplifiers and it is illustrated in Figure 1. When the input level increases beyond this point, the output signal clips and saturates. Linear amplifier needs to operate at power levels below the P1dB. Hence PA must be designed so that the P1dB is the maximum allowed output value. [1]

Back-off

In order to stay in the linear region with a high PAPR, the PA needs to be backed off to achieve enough headroom to avoid signal clipping. Back-off is used to describe how much lower the average output signal power needs to be in dBs than the compression point. The use of additional back-off results in lower power efficiency as the maximum efficiency is achieved when the PA operates at saturation point. When operating in the back-off region, the PAE of the PA drops notably, especially on average power levels. The back-off region of the PA is demonstrated in Figure 1. [2]

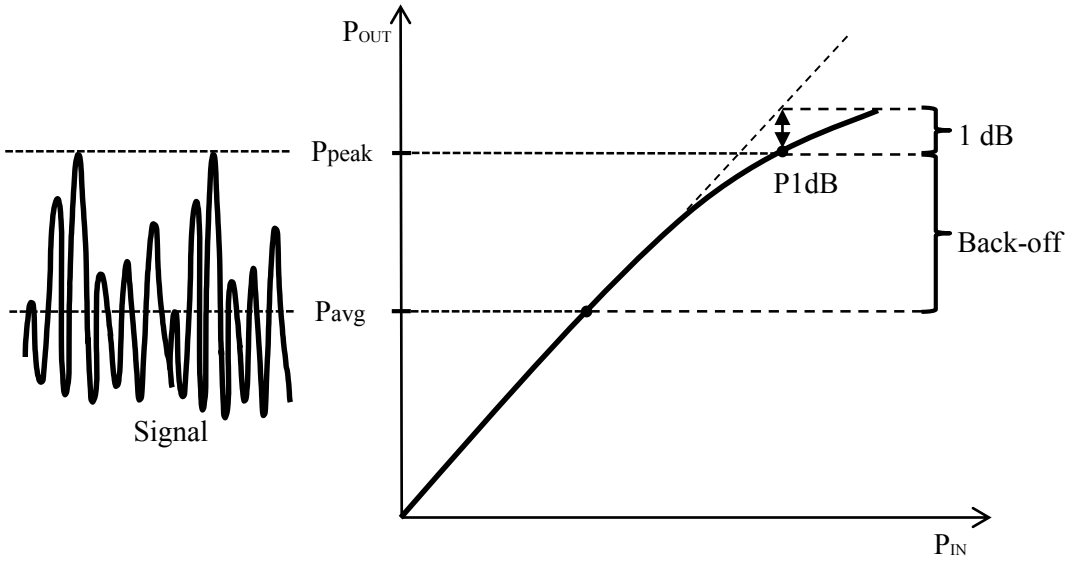

Figure 1. 1 dB compression point, back-off, and peak and average powers compared to signal waveform

2.2. Nonlinearities

Like all amplifiers the RF PA is nonlinear and when operated under large-signal condition it generates two types of unwanted tones; intermodulation products and harmonics of the carrier frequency.

2.2.1. Harmonic Distortion

The nonlinear relationship between the output voltage (v_o) and the input voltage (v_s) of a nearly-linear PA, such as a Class A amplifier, can be expanded into Taylor series around the operating point

$$v_o = f(v_s) = V_{O(dc)} + a_1 v_s + a_2 v_s^2 + a_3 v_s^3 + a_4 v_s^4 + a_5 v_s^5 + \cdots, \quad (3)$$

where $V_{O(\mathrm{dc})}$ is the DC-component of the output signal. Term a_1 is the linear small-signal gain for the fundamental input signal and a_2, a_3, … a_n are coefficients for 2,3,…,n order nonlinearities. Taylor series takes only amplitude relationship into account whereas Volterra's power series includes also phase relationship and the effect of harmonic filtering. [7]

Harmonic tones generated at the output are integer multiples of the fundamental input frequency

$$f_n = nf_0, \tag{4}$$

where n = 1, 2, 3, … is an integer and f_0 is the fundamental frequency. Harmonics can cause interference to the transmission if a harmonic signal with large amplitude falls within the input bandwidth of another receiver. Therefore harmonics are filtered out in the transmitter, typically using low pass type output matching network and duplex filter. [6]

2.2.2. Intermodulation Distortion

When two or more signals with different frequencies are applied to a PA, in addition to the harmonics also sum and difference frequencies are generated at the output. In case of two tone input the tones at the output can be calculated by

$$f_{IM} = nf_1 \pm mf_2, \tag{5}$$

where, $n = 0, 1, 2, 3,\ldots$ and $m = 0, 1, 2, 3,\ldots$ are integers, f_1 and f_2 are the tones applied to the input, and f_{IM} is frequency component caused by Intermodulation (IM). The order of intermodulation products is the sum of absolute values of n and m. Note that some of the tones fall in the fundamental band that cannot be filtered out. In addition, some of the large IM products might occur within the bandwidth of the receiver and blocks the weak input signal from the antenna degrading the reception quality [2].

The drawback of having these products is spectrum spreading. Especially 3rd order intermodulation product can be seen as troublesome because it occurs near the fundamental frequencies. This phenomenon of spectral regrowth is called Intermodulation Distortion (IMD). The spectrum of harmonics and intermodulation products is shown in Figure 2.

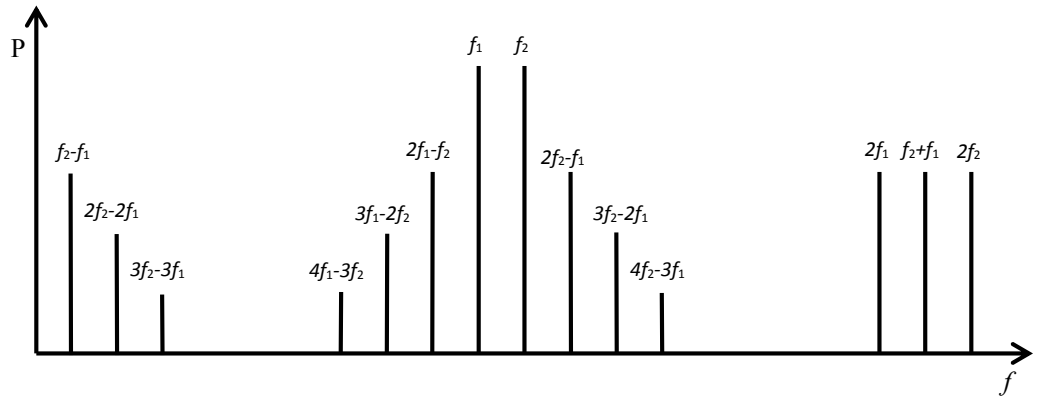

Figure 2. Harmonics and intermodulation products of frequencies f_1 and f_2.

The performance metric used to describe the linearity of the power amplifier is called Third-order Intercept Point (IP_3). It is the intersection point of extrapolated curves of fundamental signal and 3rd order intermodulation products. The horizontal coordinate is called Input IP_3 (IIP_3) and vertical is called Output IP_3 (OIP_3). Intercept points are presented in Figure 3. Intermodulation distortion in power amplifiers is

caused by operating near the compression point. IMD can be reduced by increasing back-off, so that the power amplifier is operating in a more linear region but as the trade-off efficiency is reduced. [6]

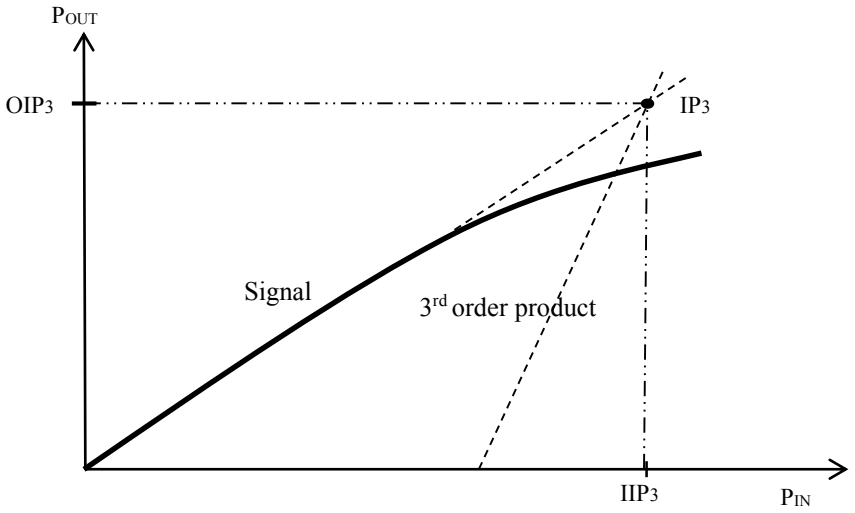

Figure 3. Third-order intercept point of the power amplifier.

2.2.3. AM-AM and AM-PM Distortion

Other important characteristics of nonlinearity in the RF PAs are the Amplitude-to-Amplitude (AM-AM) and Amplitude-to-Phase (AM-PM) distortions. As illustrated already in Figure 3, AM-AM distortion is a result of gain compression e.g. saturation (also gain expansion causes AM-AM). Phase distortion on the other hand is referred to as AM-PM distortion. It describes the phase variation at the output signal as a function of input drive. Both AM-AM and AM-PM distortions can be minimized by use of linearization methods such as digital pre-distortion. [2]

2.2.4. Adjacent Channel Leakage Ratio

The nonlinearity of the PA results in the spectral regrowth, i.e. the spectrum at the output of the PA is spread over significantly. The adjacent channel leakage ratio is essential measure to verify that the transmitter does not cause unwanted interference to adjacent transmission channels. The nonlinear behavior of the real, non-ideal power amplifier causes the signal to spread to a wider bandwidth. Especially 3rd order intermodulation distortion in multicarrier transmission causes spectral regrowth and it is unacceptable but inevitable in transmission.

The adjacent channel leakage ratio is determined as the ratio between the desired signal power on an assigned frequency channel and the power on the adjacent frequency channel. The spectral regrowth to adjacent frequency channels is illustrated in Figure 4. High ACLR means that power from the main channel is leaked into the channels next to it. The leaked power results in interference to other systems using these frequency bands and weakens the efficiency of the transmission due to spilled spectral power. While ACLR is mainly dominated by AM-AM distortion, AM-PM

distortion has disruptive effects on the transmission especially in signals with phase modulation.

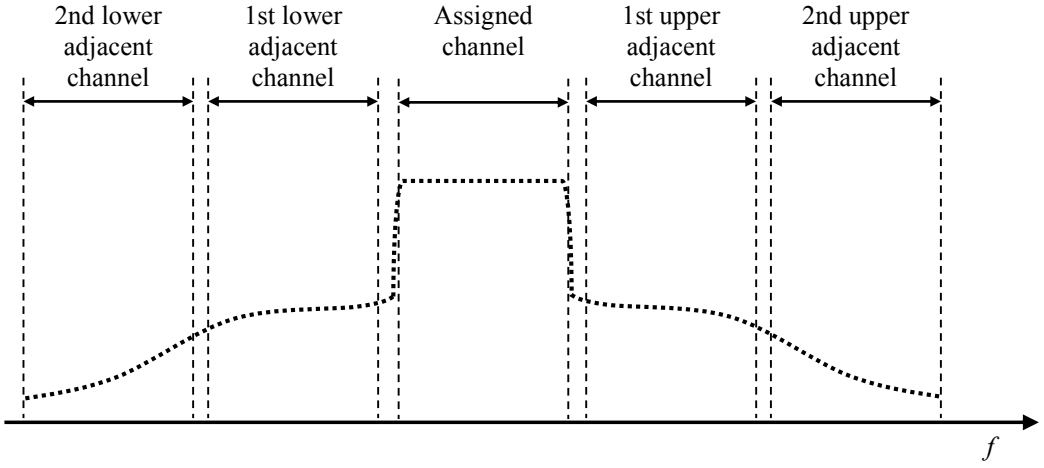

Figure 4. Spectral regrowth of the signal to adjacent channels.

2.3. Efficiency and Biasing of PA Classes

Power amplifiers are divided into classes by the conduction angle (θ) of the collector current of the transistor. Different classes have differently varying efficiency and linearity. In PA classes A, B and AB, mostly used in RF solutions, the transistor is operating as a dependent current source. Deep Class AB PA is commonly used in battery powered mobile devices due to its linear properties and relatively good efficiency.

The operating point of the PA is called the quiescent point (Q-point). It is the steady-state DC-voltage or -current at the collector of the transistor when there is no input signal. Different PA classes have different Q-point. Figure 5 demonstrates collector current (I_C) of the transistor versus collector voltage (V_{CE}) for various base current (I_B) values. The loadline is plotted to the figure to illustrate a particular load resistance (R_L). The point where the loadline intersects the base current curve is referred to as the saturation point. At this point the transistor current I_C is at the maximum and V_{CE} is at the minimum level. The cut-off point is in the intersect point of the loadline and the collector voltage axis. At cut-off point the transistor does not conduct, i.e. the collector current is zero. The Q-points of different PA classes are also presented in Figure 5. [8]

The operating point of the PA has typically a direct relation to the ACLR. Due to the intermodulation products, the leakage is increased dramatically when the PA is driven beyond its linear region at the high power levels. Typically PAs are designed so that they operate near P1dB in order to achieve maximum efficiency. Below this point the efficiency drops rapidly. However due to high PAPR in LTE the PA needs to have enough back-off from saturation so that the peak output power of the UE does not force the PA beyond the saturation. [1]

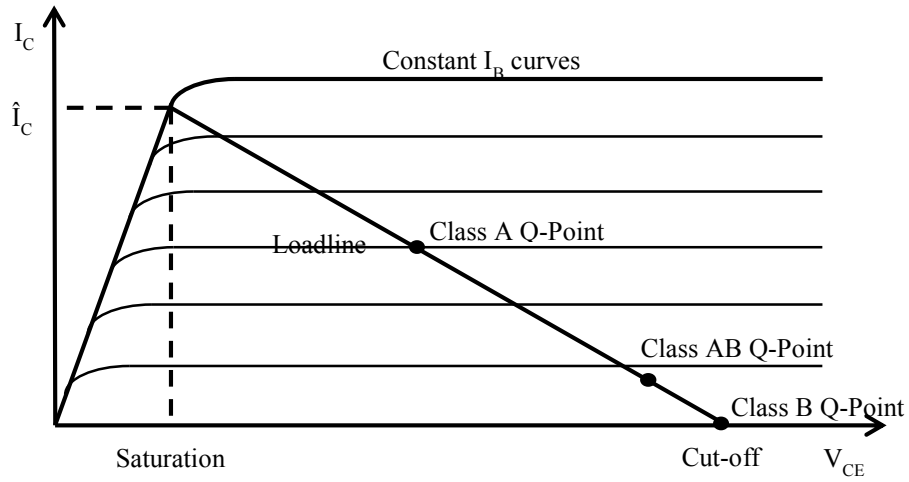

Figure 5. Loadline and quiescent point of Class A, B and AB PA.

2.3.1. Class A Amplifier

The Class A RF power amplifier is linear, which means it conducts full 360 degrees ($\theta = 2\pi$) replicating the whole input signal waveform to the output. The quiescent point is halfway between operating voltage and threshold voltage of the transistor, so the output of the device never reaches cut-off or saturation. This results in poor efficiency as the transistor is in conducting state all the time. Theoretical efficiency of a Class A power amplifier is 50% so it is not a good choice for mobile devices with limited battery capacity. [2]

2.3.2. Class B Amplifier

The Class B has conduction angle of 180 degrees ($\theta = \pi$) so it conducts only half of the input wave cycle and the Q-point is at cut-off. During the other half the transistor is turned off, meaning it can operate more efficiently but at the same time linearity is decreased notably with harmonic distortion. One half of the modulated signal wave includes the phase and amplitude information required for data transmission. Continuous form of the wave is formed with resonant circuit at the output, which provides the missing half-cycle when the transistor is off [4]. The theoretical peak efficiency of a Class B PA increases up to 78.5% when the transistor is operating half of the time compared to Class A PA [2]. The efficiency also decreases more slowly with decreasing amplitude than it does in Class A.

The quiescent point is determined so that collector current is zero when the transistor is not operating. This results in better efficiency compared to Class A PA but with the cost of degraded linearity. Class B PA has even order harmonic distortion due to output signal clipping.

2.3.3. Class AB Amplifier

To avoid discontinuity of the signal, a strict Class B amplifier is seldom used in RF solutions. In Class AB the conduction angle is between 180 and 360 ($\pi < \theta < 2\pi$), and as the name suggests it is an intermediate class between Class A and Class B. Also the efficiency is in between these two. Trade-offs between linearity and power efficiency can be varied with proper biasing of the amplifier circuit. Class AB often offers a wider linear dynamic range than either Class A or B. [7], [8]

Most linear RF power amplifiers in mobile devices are operating in moderate Class AB. This is because Class A PA is not efficient enough and practical realization of Class B is limited. Sufficient linearity can still be achieved with Class AB biased to the peak output power level, because in a typical modulation system with a variable envelope the actual power output level is mostly smaller than the peak level. While ideal Class AB is not actually linear, in real life it often provides the best linearity for variable envelope signals in mobile devices compared to other classes. [6]

2.4. Efficiency Improvement

The PA classes were compared in terms of linearity and efficiency in Section 2.3. Techniques to enhance the efficiency of the case-specific PA have been developed. The most commonly used method in mobile devices is supply voltage variation in proportion to transmit power. If the supply voltage of the PA is optimized continuously the efficiency is increased and thermal effects are reduced compared to fixed supply voltage. The operation point of the PA can also be varied resulting in more linear behavior. Load impedance is typically tuned so that an optimal output power, linearity and efficiency are achieved.

2.4.1. Average Power Tracking

Average power tracking uses the output transmit power to determine the proper supply voltage in the collector of the transistor so that the efficiency is improved, while linearity is preserved. Collector voltage of the transistor is regulated from battery voltage using a power efficient DC-DC converter. Voltage values are predetermined for every power level so that linearity of the PA is maintained on a whole operating bandwidth.

Changing the supply voltage of the power amplifier, so that it operates as close as possible to the compression point, maximizes the efficiency achieved by supply voltage variation. The APT adjusts the supply voltage according to transmitter output power between every 3GPP specified LTE slot time (0.5 ms), which is quite slow. In fact, the supply voltage is adjusted at the same pace as the UE output power in the transmission. APT also supports variation of quiescent current (I_{QC}) according to output power to allow more options for efficiency improvement. Supply voltage and quiescent current can be specified briefly for each power level typically with 1 dB resolution. [9]

2.4.2. Envelope Tracking

The next step in efficiency improvement with supply voltage variation is envelope tracking. It is faster and more accurate compared to APT as it adjusts supply voltage in real time according to PA input signal. The solution is however more complicated than APT as it requires a separate or integrated envelope tracking module, which not just increases component count and impedance matching complexity, but also requires more tuning to achieve improved efficiency [3]. In Figure 6, envelope tracking and average power tracking modulated PA supply voltages are compared to a situation where supply voltage is kept fixed. The power saving achieved with APT compared to fixed voltage is marked with darker grey. Light grey area shows further power savings with ET over APT. The excess power is dissipated as heat.

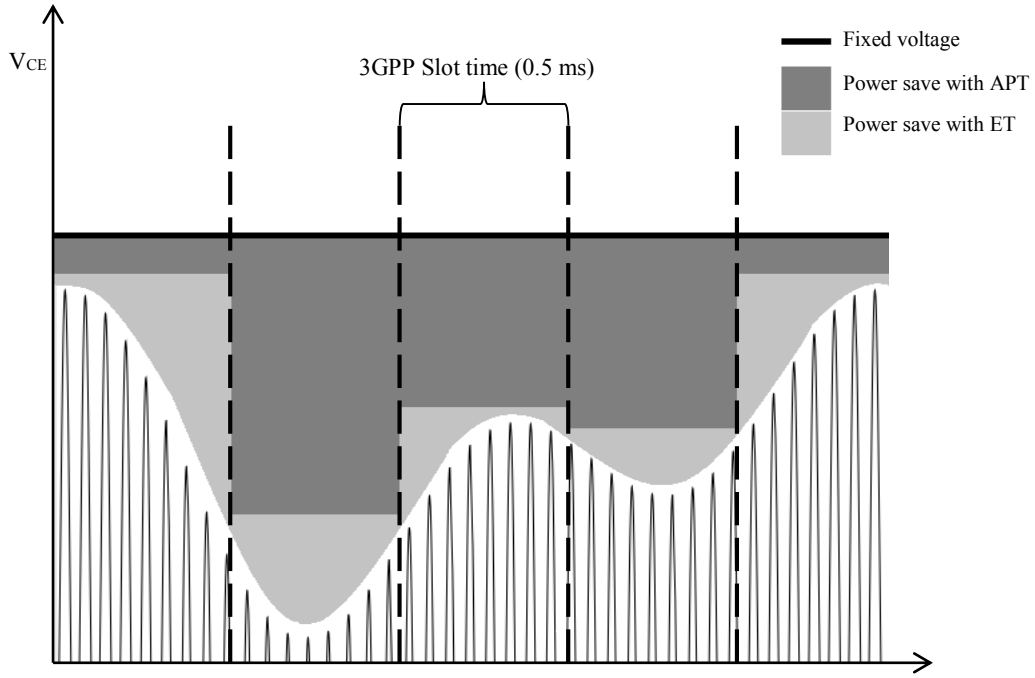

Figure 6. Power saving with use of APT and ET compared to fixed voltage

2.4.3. Quiescent Current

The effects of having different Q-point were introduced in Section 2.3. Typically the quiescent current of the PA can be tuned digitally in modern multimode power amplifiers. Varying the collector quiescent current level and Q-point can be used to improve the power-added efficiency of the PA while keeping the required linearity, especially on lower power levels. If I_{QC} is reduced on high power levels also the linearity and gain are reduced. This is why it should be used only on low power levels and changing the quiescent current of the transistor is one possibility, yet simple way to implement Low Power Mode (LPM) for the PA. A typical commercial multi-mode PA has an option to set mode and power level specific quiescent currents in order to achieve low current consumption and required performance. [6]

3. LTE TRANSMISSION AND REQUIREMENTS

The 3rd Generation Partnership Project [5] has defined a set of minimum radio frequency performance requirements for user equipment in Evolved Universal Terrestrial Radio Access (E-UTRA), which is the air interface for 3GPP Long Term Evolution devices. These requirements are an essential part of the LTE standard. The performance requirements guarantee consistent and predictable performance of the system in an environment where multiple manufacturers and vendors are involved. The relevant specification concerning this thesis is 3GPP TS 36.101 Evolved Universal Terrestrial Radio Access; User Equipment Radio Transmission and Reception [5].

3.1. Transmit signal properties

LTE uses Orthogonal Frequency Division Multiple Access (OFDMA) in downlink and Single Carrier Frequency Division Multiple Access (SC-FDMA) in uplink for multiple access scheme. Transmission bandwidth in LTE is scalable from 1.4 MHz up to 20 MHz. These multiple access solutions improve the capacity of the network and reduce interference because of orthogonality between different users. LTE supports Quadrature Phase Shift Keying (QPSK) and 16-symbol Quadrature Amplitude Modulation (16-QAM) modulations in uplink. In addition, 64-QAM is also supported in downlink. Both OFDMA and SC-FDMA multiple access schemes are presented in Figure 7. [10]

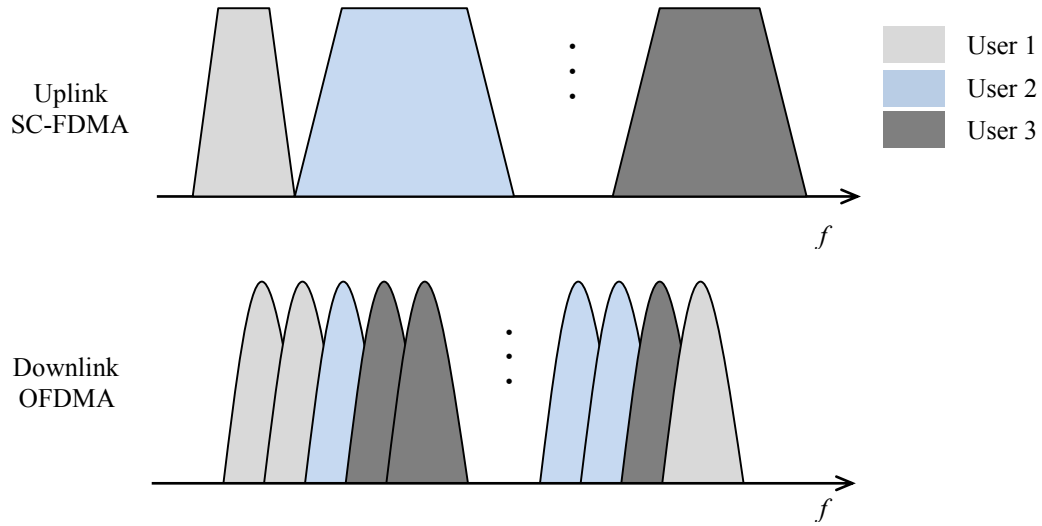

Figure 7. Illustration of multiple access schemes for downlink and uplink in LTE.

LTE transmission is based on 10 ms radio frames. These frames are divided in 20 equally sized 0.5 ms slots. Transmission bandwidth in both uplink and downlink is divided into 180 kHz wide Resource Blocks (RB) which consist of contiguous subcarriers with 15 kHz spacing. In time domain one RB corresponds to one slot time of 0.5 ms. For uplink the allocation of resource blocks needs to be continuous to enable single carrier transmission. In downlink, RBs can be allocated freely on different parts of transmission spectrum so they don't necessarily have to be adjacent to each other.

The RB size of 12 subcarriers is the same for all LTE bandwidths and the relationship between channel bandwidths and resource blocks is presented in Table 1. [10]

Table 1. Maximum resource blocks and measurement bandwidths for different LTE channel bandwidths [5]

Channel Bandwidth	Maximum resource blocks	Measurement Bandwidth
1.4 MHz	6	1.08 MHz
3 MHz	15	2.7 MHz
5 MHz	25	4.5 MHz
10 MHz	50	9.0 MHz
15 MHz	75	13.5 MHz
20 MHz	100	18.0 MHz

In Figure 8 it is presented how resource blocks fill the channel bandwidth of one E-UTRA carrier. Measurement bandwidth is 90% of the channel bandwidth for all transmission bandwidths except 1.4 MHz channel bandwidth, which uses 77 % of the transmission. Transmission bandwidth is determined by the amount of active resource blocks used for the signal transmission. [5]

In OFDMA subcarriers are modulated independently with data symbols. Modulating high rate symbols to lower rate subcarrier with long symbol duration allows the transmission to be more robust against multipath propagation of the radio channel and reduces inter-symbol interference (ISI) at the receiver. Typically ISI is caused by multipath propagation when symbols are interfering with subsequent symbols. The OFDMA transmission consists of parallel, modulated signals in the frequency domain which corresponds to multiple sinusoidal waves with different frequencies in time domain. This causes the signal envelope to vary strongly and the momentary sum of sinusoids leads to Gaussian-like distribution of different peak amplitude values and eventually high peak-to-average power ratio. [10]

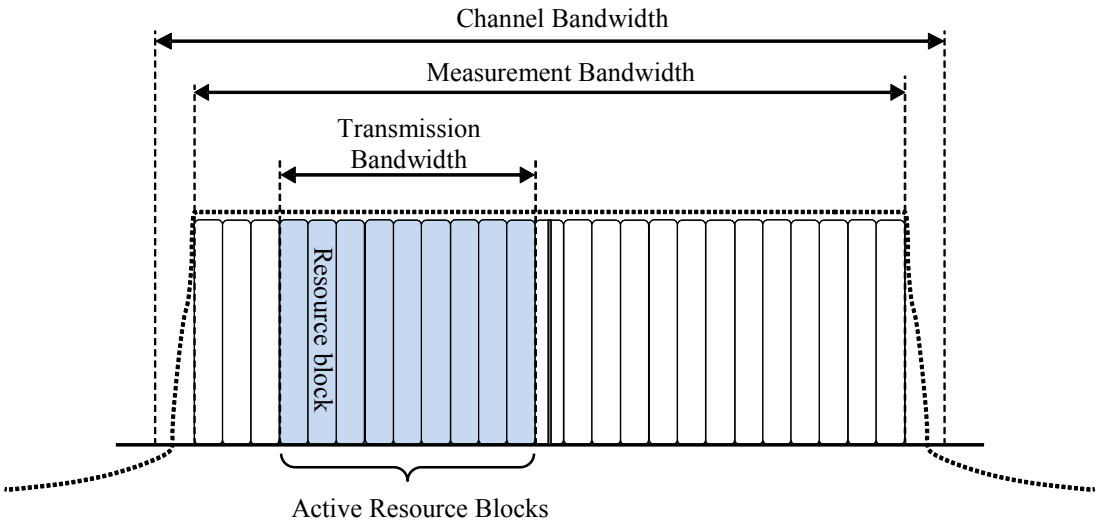

Figure 8. Definition of channel bandwidth, measurement bandwidth and transmission bandwidth for one E-UTRA carrier.

SC-FDMA differs from OFDMA with an additional Discrete Fourier Transform (DFT) block in the signal generator chain, thus it can be described as a pre-coded OFDM scheme. The DFT is placed before dividing the symbols into subcarriers resulting in that symbols are divided across all subcarriers in the frequency domain. This procedure decreases the amplitude envelope variation among subcarriers, resulting in significantly lower PAPR compared to OFDMA. However, it suffers from ISI that can be canceled by applying cyclic prefix (CP) to the carrier. The comparison between PAPR values of OFDMA and SC-FDMA is done in multiple publications, for example [11], [12], and depending on the modulation and the number of resource blocks, the SC-FDMA has several decibels lower PAPR than OFDMA.

Handling signals with high PAPR is not a problem for base stations, but for linear power amplifiers used in mobile devices with limited battery capacity, high PAPR signals are not ideal because of degraded efficiency and poor battery life. This is the main reason why 3GPP chose SC-FDMA to be used as the multiple access scheme for uplink. [5], [13]

3.2. Transmitter Requirements

The 3rd Generation Partnership Project Release 9 technical specifications describe the requirements for UE transmission. The 3GPP specified maximum output power for LTE user equipment is 23 dBm with a tolerance of ±2 dB for all operating frequency bands. The minimum controlled output power of the UE is specified to be at least -40 dBm for all channel bandwidth configurations. The duration of measured maximum and minimum output power is at least one sub frame (1 ms). [5]

3GPP has also specified requirements for behavior outside the assigned bandwidth as LTE transmission should not interfere with other existing systems. The spectrum of UE transmitter output consists of the emissions on the occupied channel bandwidth, Out-of-Band (OOB) emissions and far out spurious emissions. The out-of-band emissions are unwanted emissions located right next to the assigned channel bandwidth and are mainly the result of the modulation process and the non-linearity of the transmitter power amplifier. The requirements for the out-of-band emissions are specified in the form of ACLR and Spectrum Emission Mask (SEM), which provides detailed limits for spectrum of the transmitted uplink signal up to 25 MHz from transmission channel edge.

The 3GPP spectrum emission mask specification with limits in dBm for every E-UTRA channel bandwidths is presented in Table 2. It applies to frequencies starting from both sides of the edge of the assigned E-UTRA channel BW marked as Δf_{OOB}. The channel edges are defined by the lowest and highest frequencies of the transmission band. SEM is measured with different resolution bandwidths depending on how large the bandwidth difference from the channel edge is. Immediate frequencies up to 1 MHz next to the assigned frequency channel are measured with a high resolution filter of 30 kHz bandwidth and beyond that up to 25 MHz, a measurement filter of 1 MHz resolution is used. Frequencies above the maximum value of Δf_{OOB} are considered as the spurious domain. Figure 9 shows how channel bandwidth, OOB domain and the spurious domain are located in E-UTRA frequency band.

The spurious domain consists of spurious emissions that are caused by transmitter effects such as harmonics and parasitic emissions, intermodulation, and frequency conversion products. In this thesis the contemplation of the spurious domain is left out

as the most relevant and critical nonlinear effects of the RF power amplifier can be seen on out-of-band domain. [10]

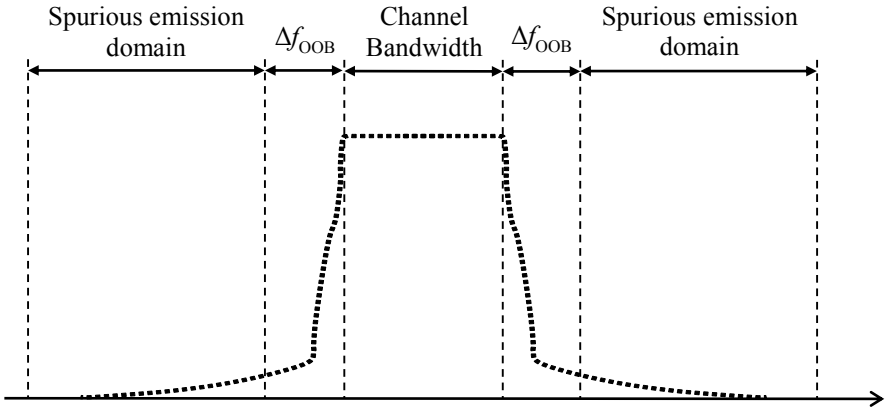

Figure 9. Definition of domains in transmitter RF spectrum.

Table 2. General E-UTRA spectrum emission mask requirements in dBm for different channel bandwidths [5]

Δf_{OOB} (MHz)	**1.4 MHz**	**3.0 MHz**	**5 MHz**	**10 MHz**	**15 MHz**	**20 MHz**	**Measurement bandwidth**
± 0-1	-10	-13	-15	-18	-20	-21	30 kHz
± 1-2.5	-10	-10	-10	-10	-10	-10	1 MHz
± 2.5-2.8	-25	-10	-10	-10	-10	-10	1 MHz
± 2.8-5		-10	-10	-10	-10	-10	1 MHz
± 5-6		-25	-13	-13	-13	-13	1 MHz
± 6-10			-25	-13	-13	-13	1 MHz
± 10-15				-25	-13	-13	1 MHz
± 15-20					-25	-13	1 MHz
± 20-25						-25	1 MHz

Adjacent channel leakage ratio requirements are specified separately for E-UTRA and Universal Terrestrial Radio Access (UTRA), which is the air interface for Universal Mobile Telecommunications System (UMTS). 3GPP General requirements for E-UTRA ACLR are presented in Table 3 and the limits are in decibels relative to carrier power (dBc). The assigned and adjacent E-UTRA channel powers are measured with rectangular filters with measurement bandwidth specified in Table 3. For LTE-LTE coexistence the E-UTRA$_{ACLR}$ limit is specified only to the same E-UTRA bandwidth to avoid an impractical amount of measurement tests resulting from mixed cases of bandwidths for the victim carrier e.g. 5 MHz to 20 MHz bandwidth. Only one adjacent channel is included in the E-UTRA ACLR specification, whereas the ACLR specification for UTRA includes two adjacent channels. [10]

Table 3. General requirements for E-UTRA$_{ACLR}$ [5]

Channel bandwidth	E-UTRA$_{ACLR1}$ Limit	E-UTRA channel Measurement bandwidth	Adjacent channel center frequency offset [MHz]
1.4 MHz	30 dBc	1.08 MHz	1.4 MHz / -1.4 MHz
3 MHz	30 dBc	2.7 MHz	3 MHz / -3 MHz
5 MHz	30 dBc	4.5 MHz	5 MHz / -5 MHz
10 MHz	30 dBc	9.0 MHz	10 MHz / -10 MHz
15 MHz	30 dBc	13.5 MHz	15 MHz / -15 MHz
20 MHz	30 dBc	18 MHz	20 MHz / -20 MHz

The UTRA band ACLR limits are to prevent unwanted emissions from appearing on the UTRA channels located next to the assigned E-UTRA channels. This is applied on two UTRA adjacent channels on both sides of assigned E-UTRA band, with UTRA$_{ACLR1}$ and UTRA$_{ACLR2}$. UTRA$_{ACLR1}$ and UTRA$_{ACLR2}$ are calculated as the ratio of the filtered mean power on the assigned E-UTRA band to the filtered mean power centered on the first adjacent UTRA channel and second adjacent channel respectively. The UTRA channel powers are measured with a raised-root cosine (RRC) bandwidth filter with roll-off factor $\alpha = 0.22$. The minimum ACLR requirements and measurement bandwidths for the first and second adjacent UTRA channels are presented in Table 4 and Table 5, respectively. [5] The ACLR is measured on both sides of the transmission bandwidth with center frequencies of adjacent channels ($\pm f_{ADJ}$) as illustrated in Figure 10.

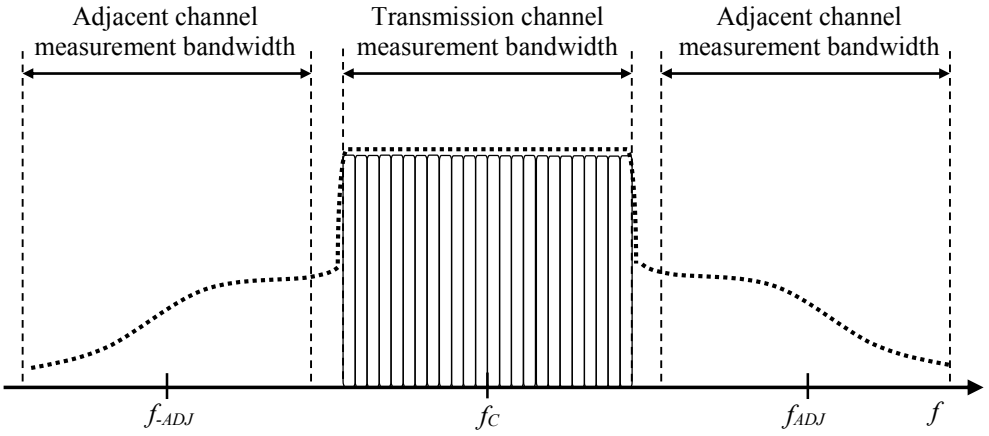

Figure 10. Transmission channel and adjacent channel measurement bandwidths used in ACLR.

Table 4. General requirements for UTRA$_{ACLR1}$ [5]

Channel bandwidth	UTRA$_{ACLR1}$ Limit	Measurement bandwidth	Adjacent channel center frequency offset
1.4 MHz	33 dBc	3.84 MHz	3.2 MHz / -3.2 MHz
3 MHz	33 dBc	3.84 MHz	4.0 MHz / -4.0 MHz
5 MHz	33 dBc	3.84 MHz	5.0 MHz / -5.0 MHz
10 MHz	33 dBc	3.84 MHz	7.5 MHz / -7.5 MHz
15 MHz	33 dBc	3.84 MHz	10 MHz / -10 MHz
20 MHz	33 dBc	3.84 MHz	12.5 MHz / -12.5 MHz

Table 5. General requirements for $UTRA_{ACLR2}$ [5]

Channel bandwidth	$UTRA_{ACLR2}$ Limit	Measurement bandwidth	Adjacent channel center frequency offset
5 MHz	36 dBc	3.84 MHz	10 MHz / -10 MHz
10 MHz	36 dBc	3.84 MHz	12.5 MHz / -12.5 MHz
15 MHz	36 dBc	3.84 MHz	15 MHz / -15 MHz
20 MHz	36 dBc	3.84 MHz	17.5 MHz / -17.5 MHz

When utilizing large RB allocations the RF power amplifier may not fulfill the linearity requirements. To avoid an impact on ACLR, it is allowed to reduce maximum output power on specific uplink transmission bandwidth configurations. Maximum Power Reduction (MPR) has been introduced to allow the reduction of transmitter output power on different modulation and bandwidth configurations. Minimum requirements of MPR are shown in Table 6. [5]

Table 6: UE Maximum Power Reduction for different channels bandwidths [5]

Modulation	**Channel Bandwidth / Active Resource Blocks**						**Maximum Power Reduction (dB)**
	1.4 MHz	**3.0 MHz**	**5 MHz**	**10 MHz**	**15 MHz**	**20 MHz**	
QPSK	> 5	> 4	> 8	> 12	> 16	> 18	≤ 1
16 QAM	≤ 5	≤ 4	≤ 8	≤ 12	≤ 16	≤ 18	≤ 1
16 QAM	> 5	> 4	> 8	> 12	> 16	> 18	≤ 2

4. FRONT-END STRUCTURE

This chapter introduces the main components used in the front-end of a mobile device. Different multiband power amplifier module architectures and their characteristics are presented. Also the power modes of the power amplifier, and how to implement them, are introduced. Other components introduced in this chapter are the Radio Frequency Integrated Circuit (RFIC), duplex filters, the antenna switch and the DC-DC converter. A simplified block diagram of a front-end structure of a mobile device is presented in Figure 11.

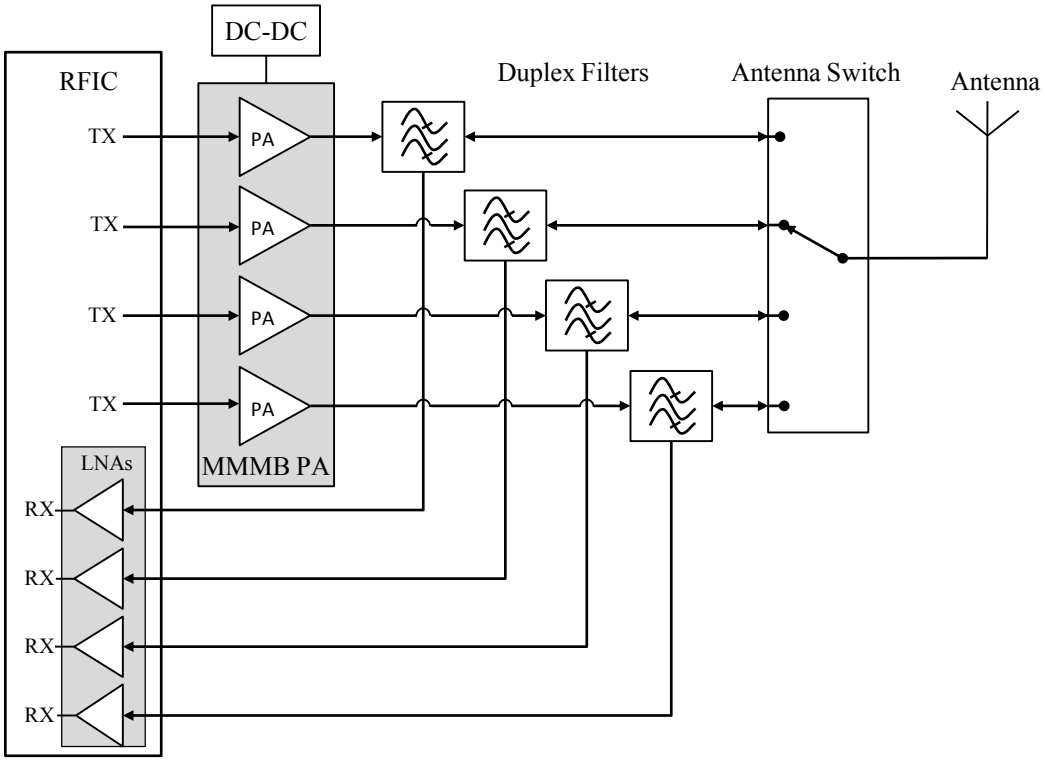

Figure 11. Simplified block diagram of the front-end of a mobile device.

4.1. RFIC

The radio frequency integrated circuit is the transceiver in mobile device. It operates as an interface between the baseband and the RF front-end. RFIC includes the Transmitters (TX) and Receivers (RX) for all supported transmission techniques with RF output ports for each operating band. The RFIC handles the mixing and up/down conversion of the baseband analog signal. In addition, output power detection from the output of the antenna port and transmit signal power management is handled in the RFIC.

4.2. Antenna Switch

The antenna switch is the component that combines all transmitter and receiver paths to the main antenna. In order to be capable of handling all the transmission techniques

and operating bands supported by the device, the antenna switch needs to be linear in wide frequency range. Both the transmitter and receiver chain have the same antenna switch and proper operating band is selected depending on the situation. The antenna switch used in a mobile device is a single pole, multiple throw design. In the transmitter the main antenna switch has several input ports for all of the operating bands supported by the device and one output port, which is connected to the main antenna. In the receiver chain the antenna switch operates in the opposite way, channeling the received signal to the RFIC. Insertion loss of the antenna switch needs to be low as it may not attenuate the amplified signal notably. The switch needs to have high isolation between the ports so that signals do not mix and the unwanted frequencies are attenuated. The low pass harmonic filters of transmitter chain for GSM bands can also be integrated into the antenna switch module.

4.3. Duplex Filter

The purpose of the duplex filter is to separate the uplink frequency range and the downlink frequency range so they don't interfere each other. In this way both can use the same antenna simultaneously. Typically uplink and downlink frequencies are close to each other thus a small shape factor is required. A duplex filter is not needed when uplink and downlink operate one at a time. The isolation between ports needs to be high enough to filter unwanted frequencies from the output ports. Also a high power TX signal can damage the RFIC if connected to the receiver chain as the RX signal level is typically below -100 dBm.

4.4. Transmitter DC-DC Converter

A DC-DC converter is used to regulate different voltage values from the supply voltage. Typically in mobile devices, a DC-DC converter is used for efficiency improvement by varying the collector voltage of the RF PA. An efficient, digitally controlled, DC-DC converter is the easiest way to apply voltage modulation to a mobile device.

A buck DC-DC converter regulates lower voltage from the supply voltage, and a boost DC-DC converter is used to regulate greater voltage from the supply voltage. A buck-boost DC-DC converter can be used when both, smaller and larger voltages compared to supply voltage, need to be generated. The voltage conversion efficiency of the DC-DC converter is crucial to the overall efficiency of the mobile device.

4.5. Power Amplifier and LNA

A power amplifier is needed to amplify the signal for the transmission. The PA needs to be linear and generate high output power as efficiently as possible. On the receiver side, Low Noise Amplifiers (LNA) are used. LNA is used to amplify very weak received signals and needs to have a low Noise Figure (NF). If the receiver chain has more than one LNA the NF of the first stage is dominating. In mobile devices the LNAs are typically integrated into the RFIC.

4.5.1. Multiband PA Architectures

As demand for higher operating band count increases, Multi-Mode Multiband (MMMB) PAs for TX are introduced. A typical MMMB PA has support for multiple LTE and Wideband Code Division Multiple Access (WCDMA) operating bands and up to four bands for Global System for Mobile Communications (GSM). Output power gain is usually 27-28 dB for LTE and WCDMA depending on the frequency band. This section introduces different MMMB power amplifier architectures and their benefits and disadvantages. Also the operation modes of the PA are explained.

Three common architectures for a commercial RF power amplifier are: discrete, where each band has its own PA, converged, where all signals of different frequency bands go through the same amplifier, and hybrid, which is a combination of the previous architectures. These architectures are designed so that GSM, WCDMA and LTE transmission technologies are covered in one solution. The MMMB architectures are presented in Figure 12.

Discrete PA architecture

The discrete power amplifier architecture is widely adopted as a front-end solution especially on today's low-end mobile devices. It consists typically of quad-band second generation systems including circuit and packet switched GSM technologies, referred as 2G, and several separate single mode power amplifiers for WCDMA and LTE standards, referred as 3G and 4G, respectively. This kind of discrete PA architecture tends to deliver the best overall transmission performance since each operating band has its own amplifier with dedicated loadline impedance and optimizations. Each PA is therefore dedicated to perform on a specific frequency band as requested. This kind of architecture however has quite a big footprint on the Printed Wired Board (PWB) space and having multiple PA modules result in a higher Bill of Material (BOM). BOM is also increased with bigger board space and matching components thus more components require more complicated routing. [4]

Converged Architecture

The converged PA module architecture was proposed to minimize the number of PA modules and paths, BOM, PWB space and wiring complexity. The module consists of two power amplifier paths, which cover both 2G and 3G/4G modes. One is for lower frequency bands (LB), with frequencies below 1 GHz, and the other is for the high frequency bands (HB) with frequencies near the 2 GHz region. These PAs are designed to support all transmission techniques and modulation standards. The loadline of the PA is set by the strictest power requirements.

The converged PA architecture reduces the number of PA paths but this comes with an expense of having degraded RF performance. This is a result of the PA having a peak output power of 33 dBm at low band frequencies with Gaussian Minimum Shift Keying (GMSK) modulation used in GSM, which is non-optimal for LTE and WCDMA modes that have 28 dBm output peak power. The dynamic range of the buck DC-DC converter is not able to provide good enough efficiency with all supported transmission techniques. A buck-boost DC-DC converter is needed to support different peak output power requirements using a different supply bias point with fixed loadline

impedances and a common output matching networks in different transmission techniques. [4]

Load switching is one option to optimize the performance of a converged PA between the two modes of operation. For higher power requirements lower impedance is shown to the collector of the PA. For techniques with lower power requirements, higher impedance is chosen. This limits the headroom in the amplifier when it is desirable. The method is not really practical in today's size requirements because of the need for multiple matching networks or shared components. This makes the design optimization more difficult for both modes. [14]

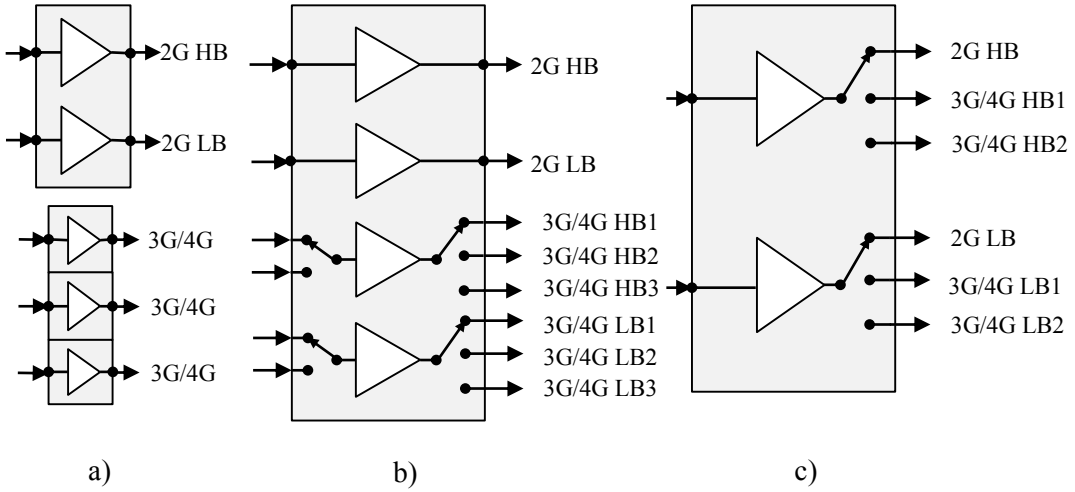

Figure 12. Multi-mode multiband power amplifier architectures. a) Discrete architecture, b) Hybrid architecture, c) Converged architecture.

Hybrid Architecture

Another, although bigger and more expensive alternative to improve RF performance compared to the converged solution is the so called hybrid PA architecture. It has a total of four PA paths, two for both 3G/4G and 2G, which eliminates the efficiency degradation issue, occurred in the converged PA architecture. One path is for high and one for low frequency bands. Broader frequency band solutions for power amplifiers are introduced in this kind of solution if one PA path is covering multiple LTE and WCDMA frequency bands. For GSM the same principle is used as in converged architecture.

The hybrid PA architecture is commonly used in today's mobile solutions with multiple LTE and WCDMA operating bands. It has excellent transmission performance, lower cost and smaller total size compared to discrete solution with dedicated PA paths and optimized loadline impedances. In Hybrid PA architecture only a buck DC-DC converter is required as each PA is optimized to its dedicated transmission technique. [4]

4.5.2. Operation Modes

Power amplifiers of today have multiple power modes to adapt to different power levels and optimize PAE. High Power Mode (HPM) can be used for all power levels

up to the maximum level. However this is not recommended on low power levels due to poor efficiency. On low power levels the current drawn from voltage supply is minimized and efficiency of the PA is increased with the use of low power mode as it is optimized for lower power levels.

The typical gain of a commercial MMMB PA for LTE with HPM is 28 dB while LPM provides 10 dB gain. Operation modes of the PA can be changed on demand. The current consumption is dropped dramatically with LPM especially when operating far in the back-off region. The linear behavior of the PA cannot be maintained on LPM when approaching the saturation point which can be seen with an increase of ACLR. The switch point to HPM is set to the maximum power level of LPM where linear requirements are fulfilled.

The PA design with HPM and LPM typically includes multiple PA stages. A design with two separate PA paths, where the other has three stages and the other has two stages, can be selected with a switch. Another technique to implement LPM is so-called stage-bypassing, which utilizes a switch to bypass the last amplifier stage. This shuts down the transistor in the last stage so that current consumption on lower power levels is decreased and thus PAE is increased. The downside of using an internal switch is extra loss and a gain difference between the power modes. [15]

In addition to stage-switching and bypassing, lower quiescent current on the transistor collector is commonly used to further improve LPM efficiency on lower power levels. This method is widely used on commercial power amplifier modules to decrease DC-power consumption, while keeping the linear performance within system requirements. Low power mode can also be implemented by adjusting the active area of the PA. This is done by disabling specific transistors in the last stage of PA design. LPM implemented this way can improve PAE with the cost of increased matching network complexity. [6]

4.6. Front-end Component Control

The RF front-end components can be controlled with a MIPI RF Front-end Control interface (RFFE). MIPI stands for Mobile Industry Processor Interface and it is developed by an open membership organization MIPI Alliance. MIPI RFFE is an industry wide standard method for controlling RF front-end components like PAs, switches and power management components. It is based on serial control logic and can be used to control various FE components simultaneously and accurately, with smaller wiring compared to the formerly popular General Purpose Input/Output (GPIO) parallel logic port interface. [16]

4.7. Front-end Impedance Matching

Other components of the transmitter consist of passive matching components such as coils and capacitors. They are used to form impedance matching networks between major FE components. Impedance matching is needed to minimize the reflections between components so that the maximum potential of the RF signal is transmitted from the RFIC to the antenna. All major front-end components typically have their input and output ports internally matched to a standard impedance of 50 ohms. Dedicated impedance matching networks are required between all FE components for every supported operating band in order to achieve the best overall RF performance.

Impedance mismatch can greatly affect the power efficiency. Trade-offs between linearity, gain and efficiency can be done with different impedance matching in order to achieve required performance.

5. MEASUREMENT SETUP

This chapter describes the structure of the measurement setup and introduces the device under test used in this thesis. Also the measurement procedure, performance measurement results of the DUT, and handling of the results are examined. This chapter explains how the optimum average power tracking table is composed for the power amplifier.

5.1. Setup Structure

The setup used to measure the performance of the DUT is shown in Figure 13. It consists of the Agilent E4438C Signal Generator, Rohde & Schwarz FSQ8 Spectrum Analyzer, Rohde & Schwarz NRP-Z11 Power Meter and two Power Supply Units (PSU), Agilent 6626A and Agilent 66319B. All the measurement equipment can be controlled remotely. A signal generator and spectrum analyzer are synchronized by sharing the same 10 MHz reference clock, which allows more precise triggering and minimizes the frequency error between the measurement equipment. The Agilent E4438C signal generator is able to generate an LTE uplink signal with custom resource block configurations along with signals using other transmission techniques. The FSQ8 spectrum analyzer has support for 3GPP E-UTRA and UTRA ACLR measurements with corresponding 3GPP specification limits. The setup is suitable for measuring individual power amplifier modules or devices with additional front-end components.

The LTE uplink signal is generated using Agilent E4438C wideband signal generator and fed directly to the input of the power amplifier. Two separately controlled power supply units are connected to the DUT. One is for generating the DC battery voltage (V_{BATT}) for the DUT, and the other power supply unit is connected to the PA, acting as bias voltage supply (V_{BIAS}). Performance of the DUT is measured with a spectrum analyzer from the output port of the antenna switch. The FSQ8 spectrum analyzer used in this setup gives the measured ACLR results as decibels in proportion to carrier power (dBc).

The spectrum analyzer is not very precise in terms of power measurement. To achieve more exact output power measurement results, the output of the DUT is connected to separate power meter with a coupler. The NRP-Z11 power meter is used to measure the power in real time from the output port of the DUT. The power meter measures the total mean power of the transmission and is considered to be more precise compared to the power measured with the spectrum analyzer as the resolution of the spectrum analyzer can be several decibels. The power level relation between main and adjacent channels from spectrum analyzer used for ACLR measurements can be considered as reasonable. The whole system is calibrated and attenuations from RF cables are calculated and taken into account to achieve proper measurement results.

Simultaneous control of measurement equipment, measurements and result handling is done with dedicated testing software. The software has support for a wide range of measurement and testing equipment. It has a versatile graphical interface for selecting parameters and, as in this case, measurement sequences along with operating band, used channels, transmission technique and other configurations. The software stores the measurement results to a single text file with all relevant information of the measurement sequence in an organized format.

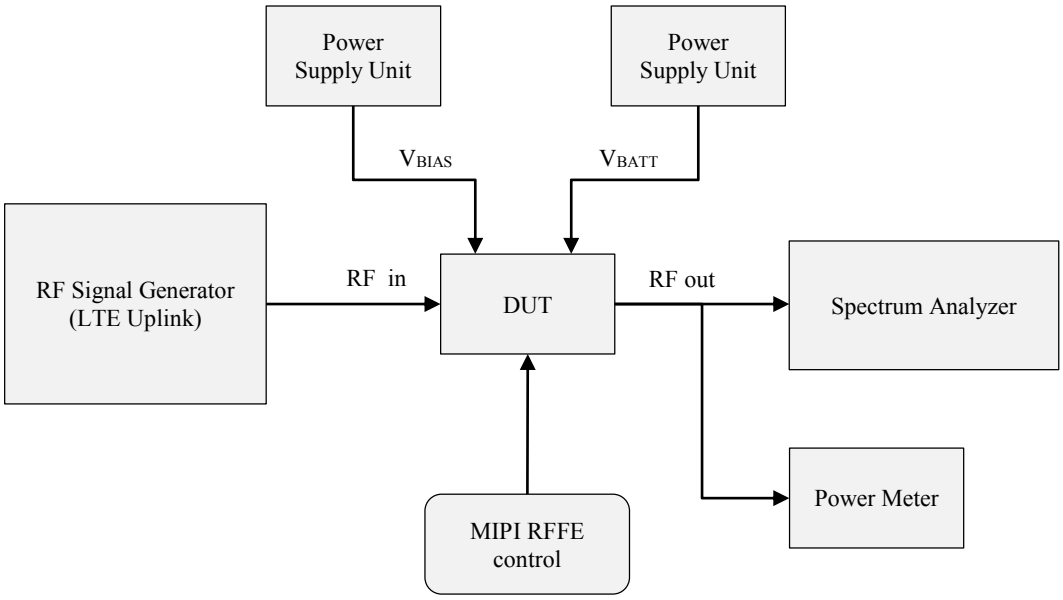

Figure 13. Block diagram of the test system.

5.2. Device Under Test

The device under test is designed so that it performs similarly to a real RF front-end of a mobile device. It consists of a multimode multiband power amplifier with hybrid architecture and duplex filters for LTE and WCDMA operating bands. It also includes a main antenna switch, which has integrated harmonic filters for high and low GSM bands. Matching networks are located in between the PA and the duplex filter, and before and after the antenna switch to minimize reflections and optimize signal transmission. An illustrative block diagram of the DUT is presented in Figure 14.

The commercial MMMB power amplifier used in measurements is designed to perform linearly in multiple operating bands, including bands 1, 2, 3, 4, 5, and 8, with LTE and WCDMA transmissions and has support for quad-band GSM. The PA has P1dB at 28 dBm in LTE transmission. The power amplifier is optimized for average power tracking in LTE mode, so it should perform as requested under the voltage optimization operation. The PA has dedicated low power and high power modes for both LTE and WCDMA. The quiescent current of the power amplifier can be adjusted for each operating band and power mode to match the specifications.

The DUT does not have a RFIC or a DC-DC converter for the PA like in RF front-end of a real mobile device. The bias voltage is supplied from the PSU simulating the regulated voltage from DC-DC converter. The other PSU provides the DC battery voltage to the PA and the antenna switch. The control of the RF front-end components of the DUT is done with the MIPI RFFE controller. The operating band needs to be selected for the PA and the antenna switch. Also the power mode of the PA is chosen with MIPI commands.

Impedance matching between the components in DUT is made as a single compromised solution between linearity, output power and efficiency, and it is kept unchanged during the measurements. It must be noted that the matching networks between components were optimized for higher power levels due to the fact that performance on lower power level is not as susceptible to variance.

The DUT has two SMA-coaxial connectors for connecting the RF cables to the testing setup. The RF input signal is fed directly on the input of the PA and the RF output signal is measured at the output of the antenna switch after the impedance matching. The ports of the power amplifier module and the antenna switch are internally matched to a standard 50 ohms as well as the coaxial connectors and RF cables in the measurement setup.

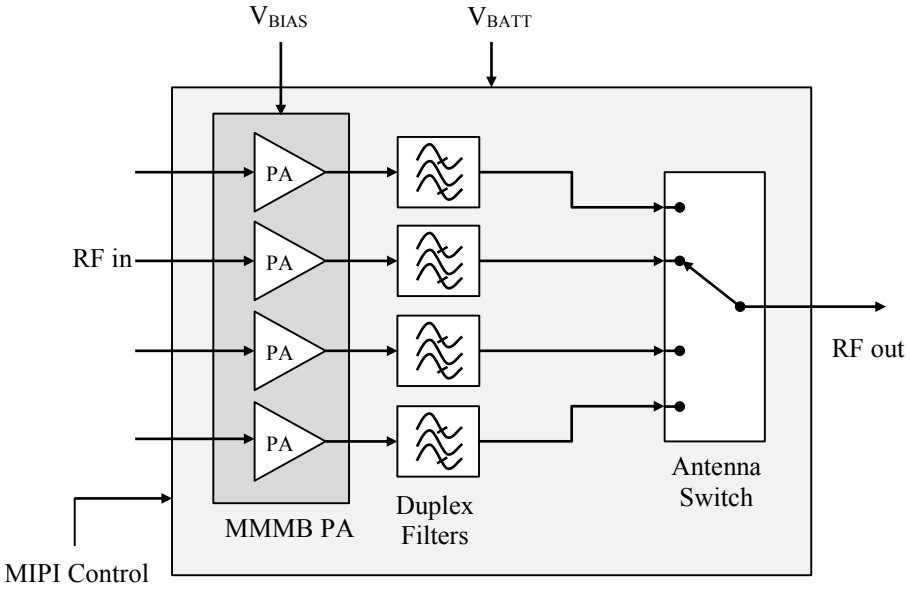

Figure 14. Simplified block diagram of the multiband transmitter chain in device under test.

In comparison to the raw PA component performance measurements, the DUT with the rest of the transmitter chain components and impedance matching networks has more similar performance to a real RF front-end chain with nonlinearities and insertion losses. The insertion loss in the DUT caused by the components after the PA is about 3 dB.

5.3. Measurement Procedure

The test sequence to measure the performance of the DUT includes mean output power measurement, with E-$UTRA_{ACLR}$, $UTRA_{ACLR1}$ and $UTRA_{ACLR2}$ measurements. Current consumption of the power amplifier is also measured. The following measurement results are used for forming the average power tracking table for the power amplifier.

A complete APT table consists of information about the output power, used bias voltage, power mode of the PA, and used operation band and channel. Some power amplifiers support a quiescent current option for each power level included in the APT table. In these measurements both PA power modes have their own different quiescent current values, provided by the component manufacturer, which are kept constant through the measurements to remove additional factors of result variation.

The signal used in measurements is a QPSK modulated SC-FDMA uplink scheme with a 5 MHz channel bandwidth and eight resource blocks. Different RB allocations

need to be measured separately, first with low allocation, where RBs are located on the lower end of the 5 MHz channel bandwidth, and then with high allocation, where RBs are on the higher end of channel bandwidth. An example of high resource block allocation is presented in Figure 15. Both RB allocation configuration measurements are done in subsequent cases and results are stored in the same file.

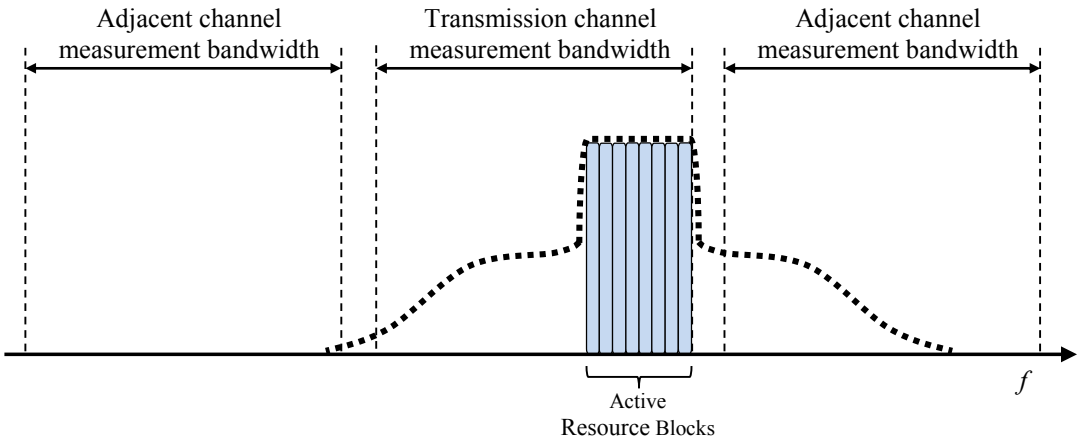

Figure 15. High resource block allocation and measurement bandwidths transmission and adjacent channels.

The transmission channel bandwidth of 5 MHz is selected due to its common characteristic as it is supported by all of the current LTE operation bands. The amount of eight resource blocks is selected because of the lack of maximum power reduction. As stated in Table 6, the MPR is not taken into account when the amount of RBs is eight at maximum on 5 MHz bandwidth with QPSK modulation. The other main reason is that eight RBs have wide enough frequency bandwidth so that IMD products land properly on the adjacent measurement channel when they are allocated near the channel edge. As stated in Table 3, the 5 MHz E-UTRA$_{ACLR}$ adjacent channel center frequency offsets are ±5 MHz and measurement bandwidth is 4.5 MHz. For example, in the case of one resource block, measurements do not give proper ACLR results as its IMD products appear180 kHz away from the carrier according to (5). The effect of high RB allocation to the ACLR results is shown in Figure 15. The spectral regrowth caused by the IMD products appear more on the adjacent channel that is closer to the active resource blocks. The measured ACLR on upper adjacent channel is greater compared to the lower adjacent channel result. The same effect is with the case of low RB allocation while more power spreads on the lower adjacent channel.

The operating band used for measurements is 3GPP E-UTRA band 2, which is supported by the PA. The frequency range of band 2 is 1850 – 1910 MHz with a middle channel frequency of 1880 MHz. The measurement procedure can be done for multiple channels and in different ambient temperatures. Usually the channels near the edge of the operating band and temperatures that differ greatly from ideal room temperature can be problematic as they typically have a degrading effect on the ACLR. Nevertheless, the measurements shown in this thesis were performed on middle channel with an ambient temperature of constant 25 °C in order to simplify results and speed up measurement time. Measurements were performed only with adjacent E-UTRA channels as they typically have the worst performance compared to the

performance of first and second adjacent UTRA channels. The average power tracking table is then formed based on the E-UTRA$_{ACLR}$ results.

For low and high power modes of the power amplifier, the whole test set is measured with different sequences and results are stored in separate files. This is because the APT table has bias voltage values defined separately for HPM and LPM and in this way the results of both power modes can be observed independently and more accurately.

The measurements used for forming the average power tracking table include the output power and ACLR measurements with various different bias voltages. Before the initialization of the measurement procedure all relevant parameters such as output power target (P_{TARG}) range and V_{BIAS} range are initialized based on user choices. In this thesis, parameters used in measurements for different PA power modes are presented in Table 7.

Table 7. Input parameters for HPM and LPM used for the measurements

PA Power mode	**HPM**	**LPM**
Bias Voltage min. (V_{MIN})	0.5 V	0.5 V
Bias Voltage max. (V_{MAX})	3.4 V	2.5 V
Power Target min. (P_{MIN})	0 dBm	-12 dBm
Power Target max. (P_{MAX})	23 dBm	10 dBm
Gain guess (G_{GUESS})	30 dB	10 dB
Bias Voltage step (V_{STEP})	0.05 V	0.05 V
Power Target step (P_{STEP})	1 dB	1 dB
Input Power max. (P_{IN_MAX})	5 dBm	5 dBm

For HPM the target output power level range is from 0 dBm to 23 dBm, and V_{BIAS} value range is 0.5 V – 3.4 V. For LPM the target power level range is from -12 dBm to 10 dBm with V_{BIAS} range 0.5 V – 2.5 V. The power targets overlap between PA power modes so that ACLR performance is measured as widely as possible on both power modes. The output power level targets were selected by the assumption that the PA with LPM can operate linearly up to 10 dBm and HPM is then used for power levels above that. The bias voltage limits for the power amplifier are specified by the manufacturer. The bias voltage step of 50 mV was selected for both power modes to achieve high resolution performance results for every selected output power level. The battery voltage is kept fixed at 3.4 V through the whole measurement procedure.

The gain guess (G_{GUESS}) values are determined on the presumption that the gain of the PA on HPM is approximately 30 dB, and 10 dB on LPM. The gain guess sets the initial signal generator power (P_{IN}). Therefore the initial value of P_{IN} is set to be 30 dB lower than current target output power P_{TARG} in HPM and 10 dB lower on LPM. Measurements are done for every specified output power level with 1 dB steps, on every bias voltage step. With every step the ACLR and current values are measured and data is stored. The maximum value of input signal power (V_{IN_MAX}) is limited by the signal generator. The signal generator in this setup can produce the selected LTE signal power up to 5 dBm with reliable precision.

The measurement procedure, which goes through all bias voltage and output power target combinations, is illustrated with the flow chart in Figure 16. The signal generator increases the LTE uplink RF signal power P_{IN} until the DUT output power P_{OUT} is at a predetermined power target P_{TARG}. Output power values are measured with the power meter. The output power P_{OUT} of the DUT is proportional to the input signal

power P_{IN} with the addition of the gain (G) of the power amplifier. P_{IN} is increased by a predetermined input power step (P_{STEP}) until the P_{OUT} is within 1 dB of P_{TARG}. To achieve the output power as close to the power target as possible, a binary search method is used for fine tuning until two subsequent output power readings, measured with the power meter, are within 0.2 decibels away from the target power.

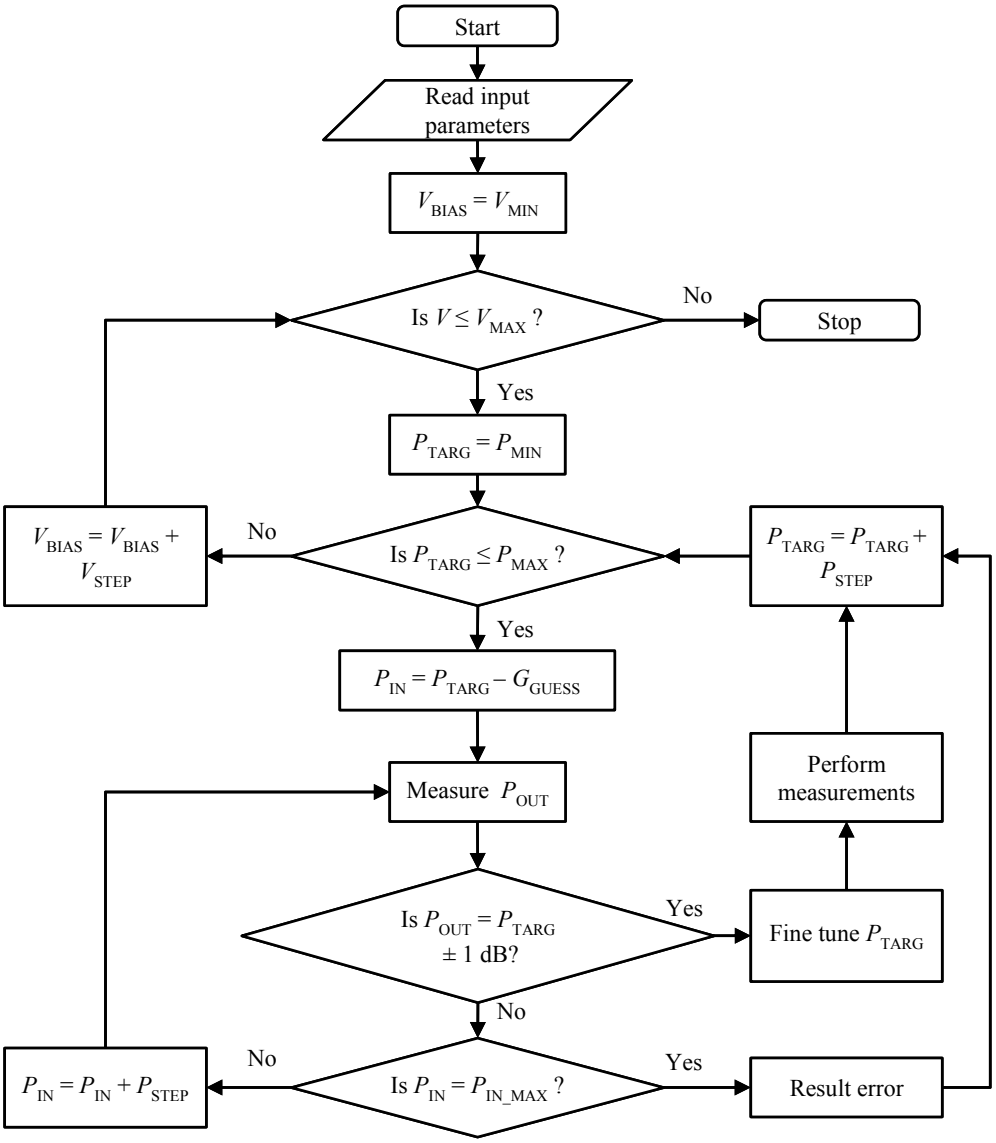

Figure 16. Flow chart of measurement process.

The measurements take place after the target output power is reached with required precision. The spectrum analyzer measures the ACLR values using an averaging of 10 sweeps. The measurement software stores the ACLR results to a result file along with input power from the signal generator and output power of the DUT from the power meter. The momentary current consumption of the power amplifier, measured with the PSU providing the bias voltage, is also stored to the same file. With these values, the total power added efficiency of the DUT can be calculated with (1). Also total gain of the DUT can be calculated simply by subtracting the input power from the output power.

After the first measurement case, the target power is increased by one step P_{STEP} and input power P_{IN} is restored to its initial value, which was defined to be corresponding G_{GUESS} below target power. The sequence is looped until P_{TARG} reaches its defined maximum value (P_{MAX}). After P_{MAX} is reached and corresponding values are measured, V_{BIAS} is increased by one voltage step (V_{STEP}) and the target power loop is restarted from its initial condition.

If the target output power is not achieved by increasing the input power from the signal generator to the maximum value (P_{IN_MAX}), no measurement is done and an error value is saved to the result file. The gain of the PA is conditional on V_{BIAS}, as lower bias voltage decreases the linear gain performance of the PA. This causes error results when P_{TARG} is not reached. In case of an error result, the measurements continue normally with the next power level step.

The whole above-mentioned measurement procedure is performed for every selected V_{BIAS} value until the maximum bias voltage value (V_{MAX}) is reached. The measurement procedure is stopped after ACLR and current values on all output power levels on every V_{BIAS} value are measured and results are stored.

The measurement system can also be used to measure ACLR on two UTRA channels. The UTRA measurement also includes the second adjacent channel power measurement. The $UTRA_{ACLR1}$ and $UTRA_{ACLR2}$ are measured in the same sequence but the $E\text{-}UTRA_{ACLR}$ measurement needs to be measured with a separate sequence due to the differentiation on the measurement bandwidths. As stated before, this chapter covers only measurements and result observations for $E\text{-}UTRA_{ACLR}$.

The measurement of all voltage and power combinations produces a great amount of result data. The data is then filtered and processed to achieve the proper, requirement fulfilling bias voltage values for the PA. The APT table file is then composed with these voltage and output power values.

5.4. Data Processing

This section describes how the optimum average power tracking table can be formed using the measurement results obtained with measurement setup introduced in Section 5.1 and the measurement algorithm explained in Section 5.3.

Due to a high amount of measurement results, the result handling and measured data processing is done with a dedicated APT optimization macro, programmed with Visual Basic for Applications (VBA). The VBA programmed macro generates an easy to review and edit datasheet with contour figures with colour scaling of the performance of the DUT in relation to output power in dBm and bias voltage in volts. The contour figures present the ACLR performance, power added efficiency of the DUT, total gain of the DUT and the current consumption of the power amplifier. These performance values are expressed with colours. The macro also generates the optimum APT table according to the measured ACLR performance form the result file. The macro is able to process both E-UTRA and UTRA ACLR measurement results and can handle result data of HPM and LPM simultaneously. The macro sorts and filters the relevant results and information from the raw data result file. The data processing macro comes into use especially when the performance of the DUT is measured on multiple channels and with different ambient temperatures.

As the performance of the DUT can vary depending on the frequency channel and different temperatures, the factors affecting the performance need to be covered. The algorithm takes the variation of ACLR, caused by the effect of channel position,

resource block allocation and different temperatures, into account separately for each power level when forming the APT table. Thus the APT table is generated according to a worst case scenario and should then satisfy all channel position, resource block and temperature configurations.

The optimum average power tracking table formation process is demonstrated with the flow chart presented in Figure 17. At first, a target value for ACLR ($ACLR_{\mathrm{TARG}}$) is provided to the APT optimization macro. The 3GPP specified ACLR requirement for LTE E-UTRA was -30 dBc [6], but in this thesis, the target for ACLR values is set to be -40 dBc providing enough margin compared to 3GPP requirements. The additional 10 dB is left for further phases of development and production which allows better productivity.

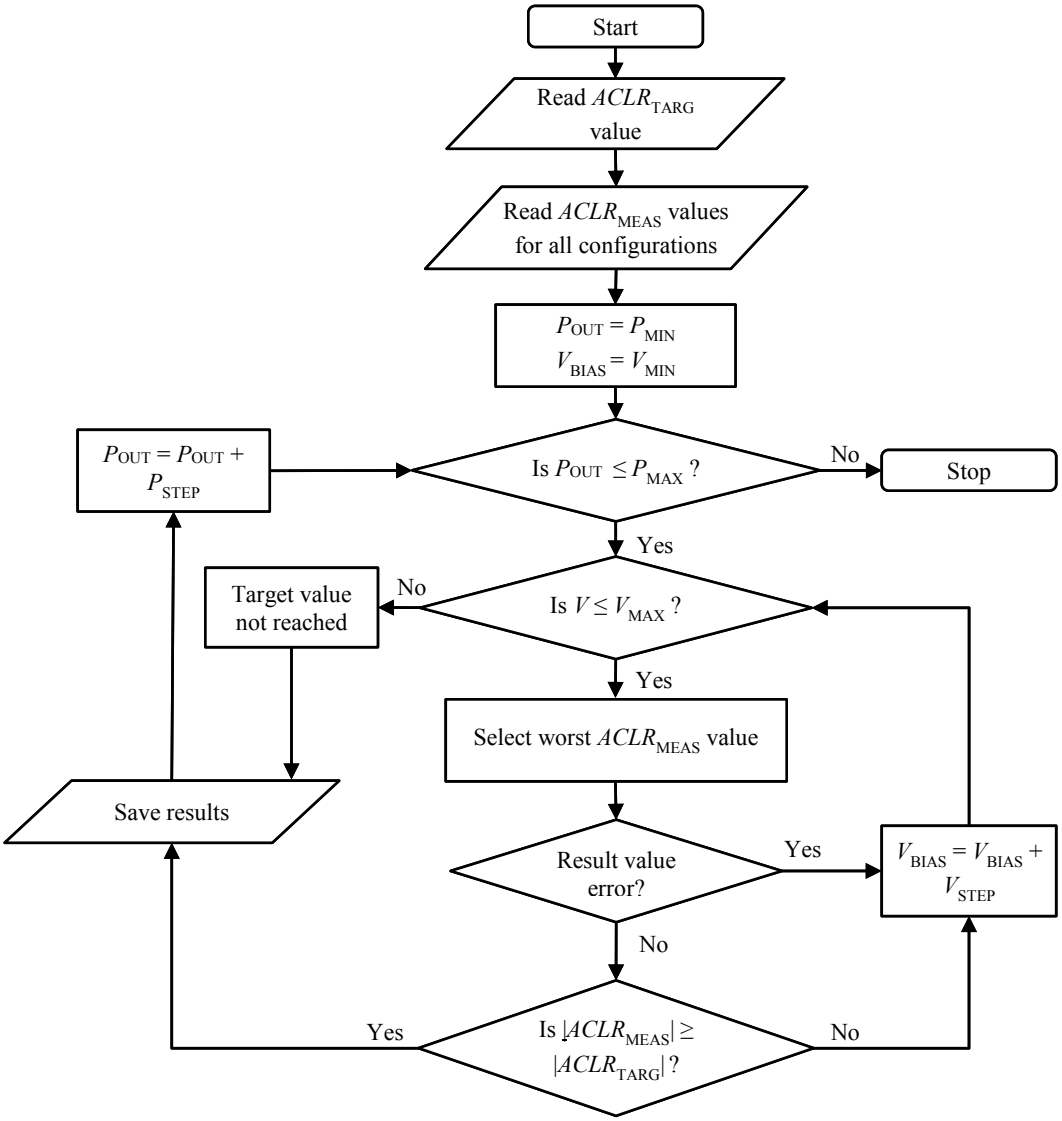

Figure 17. Flow chart of optimum bias voltage search.

The optimum bias voltage search is started with the lowest defined output power level and lowest bias voltage value. The starting point was selected based on the fact that ACLR performance increases as the bias voltage is increased. The worst measured

absolute ACLR value ($ACLR_{MEAS}$) is then compared to the predefined absolute ACLR target value to check if the measured value is valid. Absolute values are used for ensuring that both values have the same sign. Bias voltage value V_{BIAS} is increased step by step until the first measured ACLR result is greater or equal to the ACLR target value. That V_{BIAS} value is stored to the APT table to the corresponding output power value. If the ACLR target value is not reached even with the highest defined V_{BIAS} value, that voltage value is stored to the APT table with a notation which states that the ACLR result does not satisfy the requirements. This procedure is used to go through all selected power levels. The algorithm is stopped when bias voltage is found for the maximum defined output power level.

The bias voltage values selected for the APT table with the measurement algorithm can be considered as starting values and guidance for the mobile device power amplifier efficiency improvement. The voltage values of the APT table will be fine-tuned with wider performance measurements later in the product development cycle due to component performance variations.

6. MEASUREMENT RESULTS

This chapter presents the measurement results of the DUT obtained with the measurement setup introduced in Section 5.1. As stated in the previous chapter, all measurements were done on the middle channel of LTE operation band 2 at 25 °C of ambient temperature. The performance of the DUT was measured on both power modes of the power amplifier. The adjacent channel leakage ratio, power added efficiency, total gain of the DUT, and current consumption of the power amplifier are examined separately on high and low power modes of the PA.

6.1. Adjacent Channel Leakage Ratio

The most relevant measurement for the APT optimization is the adjacent channel leakage ratio, thus the APT table is formed mainly based on the ACLR performance. Figure 18 shows the performance of the device under test while the power amplifier was operating in high power mode. In Figure 18 the ACLR is presented in relation to different bias voltage and output power values. The ACLR results are in decibels relative to carrier power which results in negative values. Measured ACLR values are presented with colour contours and each colour bar defines the measurement values. Invalid measurement results and error results are shown as black.

The black line presents the optimum bias voltages for each output power level with ACLR of -40 dBc obtained with the algorithm introduced in Section 5.4. These voltages are the specific values that form the optimized average power tracking table. The same bias voltage line is also present on other contour figures so that performance of the DUT with the optimum bias voltages from the generated APT table can be easily examined.

The ACLR measurement results in Figure 18 show that the ACLR performance decreased when the requested output power was increased. This is the result of an insufficient voltage on the collector of the transistor in the power amplifier, which causes distortion to the output signal. The bias voltage of the power amplifier can be increased which results in better ACLR values on specific power levels. On lower output power levels, lower bias voltage is sufficient to provide low distortion PA performance. The need of bias voltage shows an exponential increase in order to keep the ACLR values as expected when the power is increased. The ACLR of -40 dBc was achieved for the maximum measured output power of 23 dBm with a supplied bias voltage of 3.3 V, which is below the maximum potential bias voltage 3.4 V.

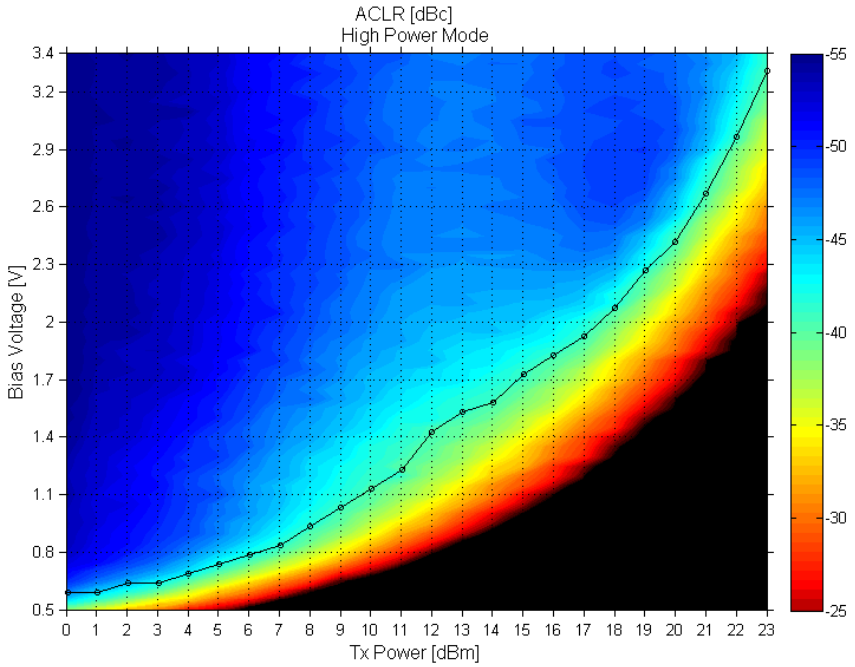

Figure 18. ACLR as function of output power and bias voltage on HPM.

The ACLR results on LPM of the PA, presented in Figure 19, show the same behavior as the HPM performance measurements. The limit line of -40 dBc for ACLR is also present. As can be seen from the figure, the value of -40 dBc is not reached on power levels above 7 dBm, even with a maximum defined bias voltage of 2.5 V. The switch to HPM needs to be done at this point at the latest to maintain the set ACLR requirements.

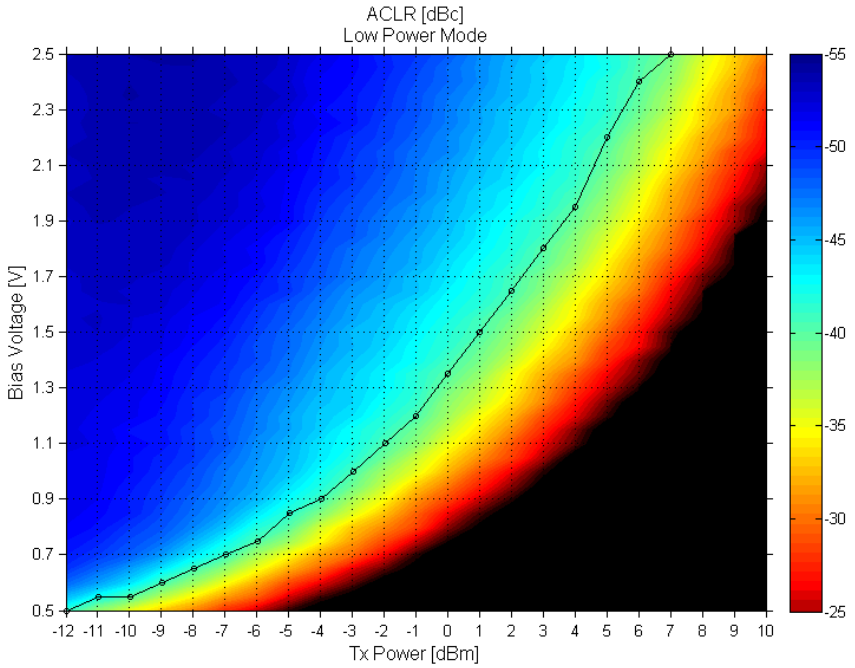

Figure 19. ACLR as function of TX power and bias voltage on LPM.

6.2. Gain

The total gain of the DUT was calculated simply by subtracting the input power from the measured output power. Based on the measurement results in Figure 20 the gain of the DUT, while the PA is operating on high power mode, can be above 25 dB on every power level if bias voltage is set to a maximum of 3.4 V. As stated before the components after the PA had about 3 dB attenuation, which gives a total of 28 dB gain to the PA on HPM.

By decreasing the bias voltage, the gain shows a rapid drop to the point where target power is not reached and an invalid result is recorded. The invalid error results can be explained with the decreased gain of the DUT, which results in unreached target output power. The signal generator limits the amount of results as the maximum linear input power from the signal generator was 5 dBm. The maximum output power 23 dBm of the DUT was not achieved with a gain below 18 dB. With higher linear power of the signal generator the lower gain performance with low bias voltage could be measured.

In Figure 20 the bias voltage line is placed on top of the contour figure. It shows that the gain of the DUT is 25 dB on high power levels with optimized voltages. The gain drops below 20 dB when output power is under 9 dBm while applied bias voltage is 1 V. This is still sufficient as the output powers were achieved by increasing the power of the input signal.

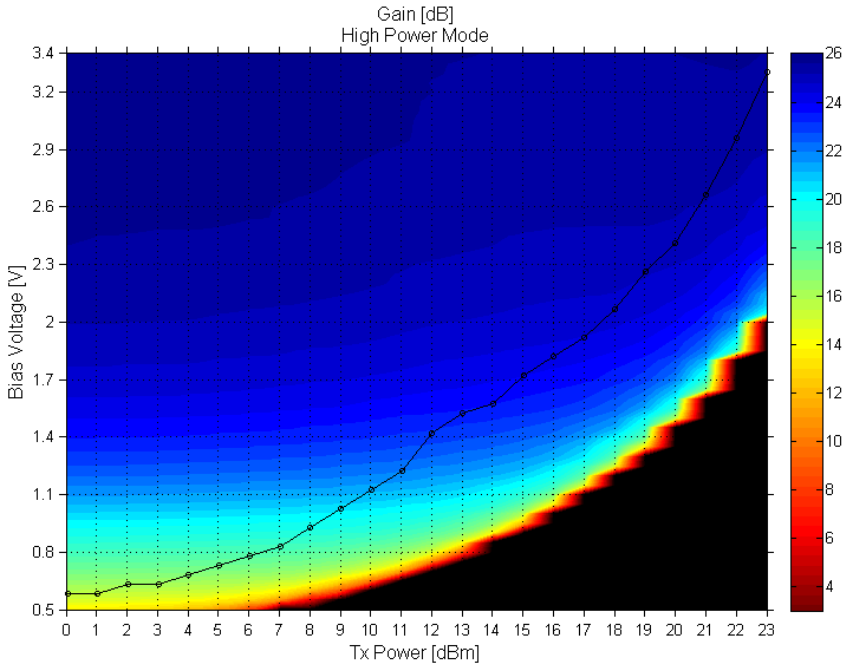

Figure 20. Total gain of the DUT with power amplifier operating on HPM.

Figure 21 shows the total gain of the device under test with the power amplifier operating in low power mode. When maximum bias voltage of 2.5 V is applied the gain of the DUT is 11 dB on all measured power levels. The behavior is similar to HPM as the gain of the DUT decreases rapidly with low bias voltages when moved to higher power levels.

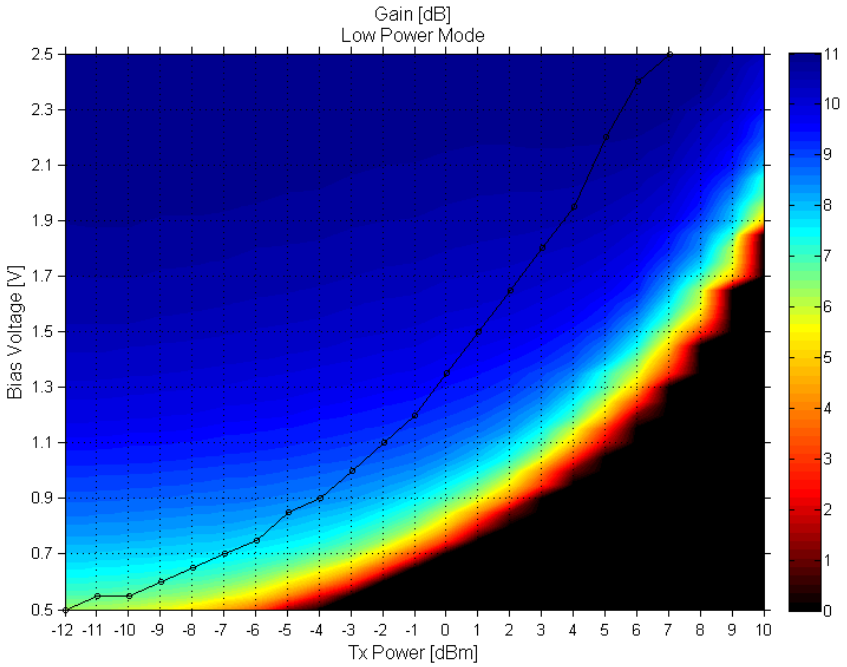

Figure 21. Total gain of the DUT with power amplifier operating on LPM.

6.3. Current Consumption

Figure 22 presents the current consumption of the power amplifier on HPM in relation to bias voltage and output power. Current is measured with the PSU, which is used to supply bias voltage to the PA. Total current consumption of the DUT was not measured due to the power amplifier being the major cause of current consumption during signal transmission.

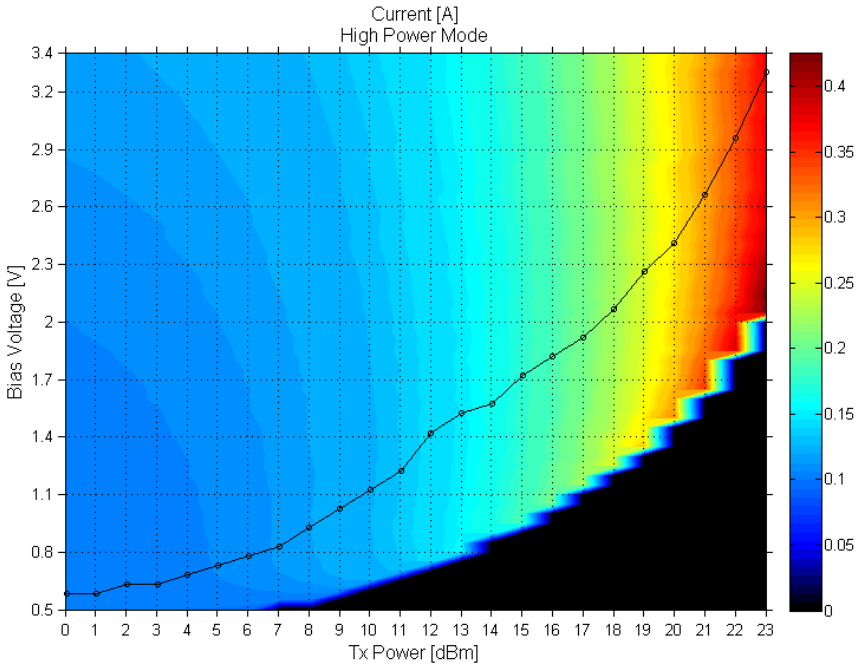

Figure 22. Current consumption of the power amplifier on HPM.

As can be seen from Figure 22, the current consumption of the power amplifier hardly depends on the bias voltage. The output power level determines the current consumption as the current demand rises as output power increases. The highest current consumption was measured at maximum output power. The voltage optimization of the power amplifier does not affect notably to the current consumption. The -40 dBc bias voltage line is marked to the figure to illustrate how the current consumption behaves on different power levels with optimum bias voltages.

Figure 23 presents the current consumption in low power mode in relation to bias voltage and output power. The pattern is the same as with HPM where the current consumption mainly depends on output power level. The current consumption of the PA in low power mode is notably lower compared to the situation when the PA is operating in high power mode.

The figures shows the benefits of the low power mode of the power amplifier as the difference in current consumption on the same output power level between the PA power modes is significant. The power amplifier draws at least over 100 mA of current in high power mode, even on lowest measured output power, while the worst case of low power mode current usage is 35 mA. The minimum current consumption in LPM is achieved on power levels below 2 dBm. On those power levels the PA draws maximum of 10 mA of current.

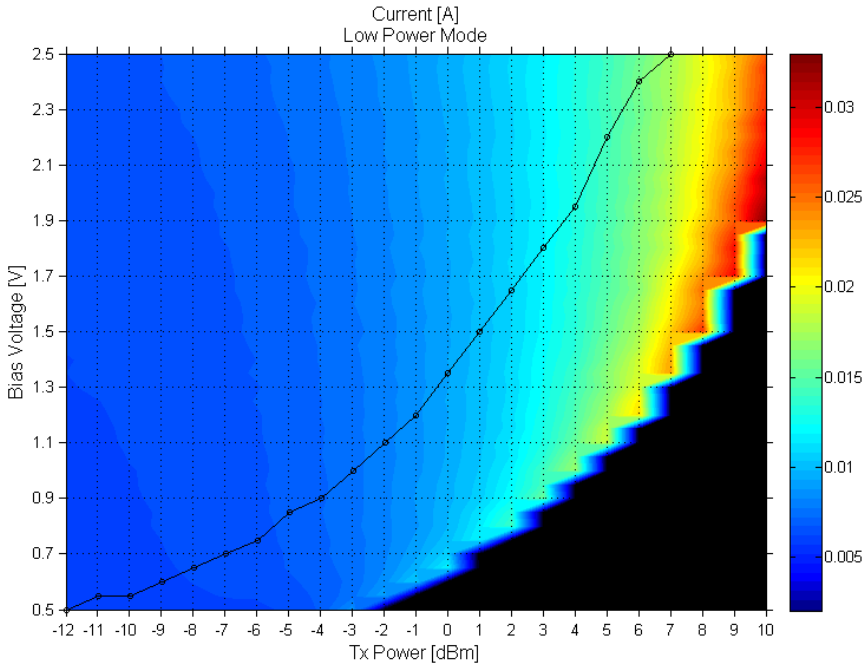

Figure 23. Current consumption of the power amplifier on LPM.

6.4. Power Added Efficiency

The power added efficiency of the DUT is calculated for every voltage and power level combination according to (1). Values used in (1) are P_{IN}, from the signal generator, and P_{OUT} from the output of the DUT. P_{DC} was calculated as a product of voltage and corresponding current values measured with the PSU providing the bias voltage to the PA.

The colour contour map of total PAE of the DUT on different power level and bias the voltage configurations with PA operating in HPM is presented in Figure 24. The DUT has a filter and antenna switch after the power amplifier in the transmitter chain. These components have about 3 dB additional loss which affects directly to the PAE. Therefore the PAE is calculated for the combination of the PA and other front-end components while consumed DC-power P_{DC} comes only from the power amplifier. The maximum measured PAE in HPM shows 20 %. The loss of 3 dB from other components equals half of the original power. When this is taken into account the power amplifier has a PAE as high as 40 % on specific bias voltages and output power levels.

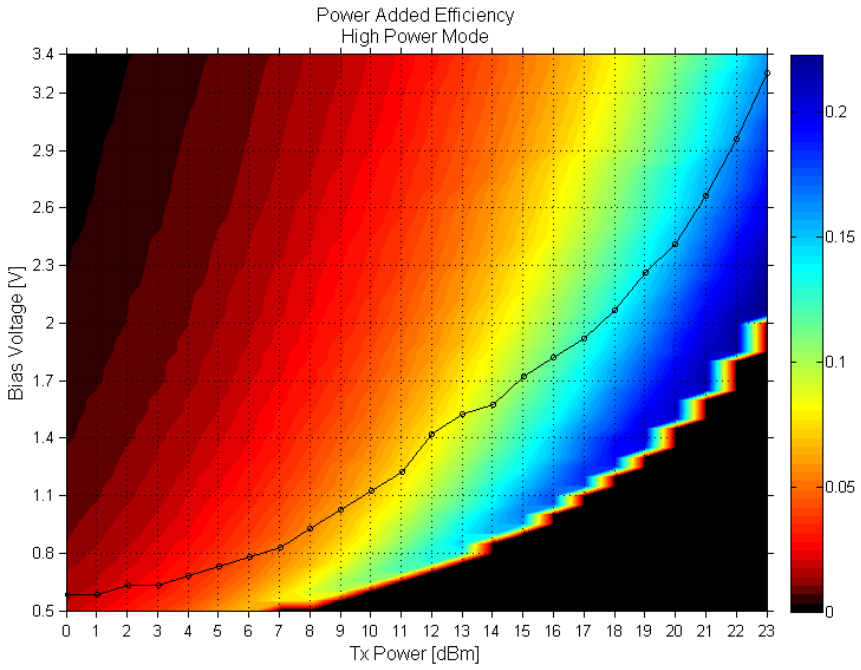

Figure 24. Total power added efficiency of the DUT with power amplifier operating on HPM.

The measured power added efficiency is worst on low power levels and with high bias voltage as expected. The best efficiency is achieved when the output power is at maximum while the bias voltage is at the lowest possible value. The best PAE is recorded on power level and bias voltage combinations that also result in poor ACLR and degraded total gain of the DUT. The -40 dBc ACLR limit line is presented on top of the PAE contour figure. It shows that the PAE increases linearly when the generated bias voltages are used. With generated bias voltages the maximum PAE of 16 % is obtained on power levels above 20 dBm. On lower power levels the PAE decreases rapidly resulting in only 5 % at 9 dBm and below.

The trade-off between linearity, efficiency and output power can also be seen from the figures. Improving the ACLR performance by increasing the bias voltage decreases the PAE of the DUT. When the output power is increased, both ACLR and PAE are decreased if bias voltage is kept constant. The ACLR sets the low limit and gain sets the upper limit for balanced performance compromise between these parameters.

Overall in comparison to a 3.4 V fixed voltage in HPM, the APT voltage adjustment increases the power added efficiency notably. With a fixed voltage, the maximum measured PAE of the DUT is 15 % at an output power level of 23 dBm, while with optimized voltages the same PAE is measured at 20 dBm.

Figure 25 presents the total power added efficiency of the DUT while the power amplifier operates in LPM. On an output power level of 10 dBm the PAE of the DUT is notably better in LPM than in HPM. But as can be noted from the ACLR limit line, the linearity requirements are not reached on power levels beyond 7 dBm. The total PAE is below 6 % up to -5 dBm. On power levels above that, the PAE grows steadily to as high as 14 %.

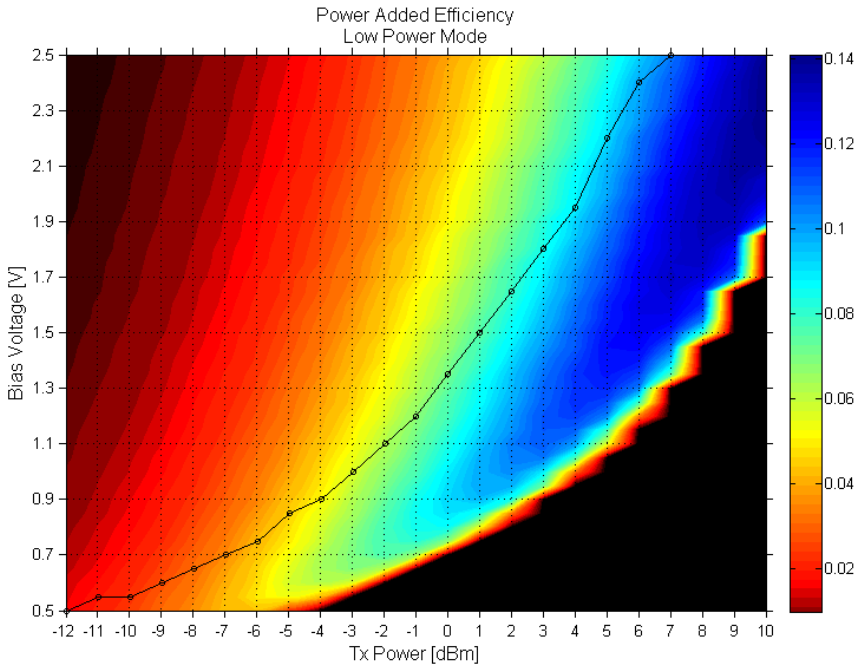

Figure 25. Total power added efficiency of the DUT while power amplifier operates on low power mode.

6.5. Switching Point

As it can be seen from the results presented above that, the bias voltages in the optimum APT table are determined by the ACLR and the PAE. The PAE can be improved by decreasing the bias voltages but that also decreases ACLR. Then again if ACLR needs to be increased the efficiency drops. The current consumption of the PA does not seem to depend on the applied bias voltage, but instead it is determined by the transmit power. The total gain of the DUT seems to remain stable with sufficient bias voltage on every power level. By decreasing the voltage the gain drops rapidly until it is insufficient to provide enough amplification for the power target. These measurements show that the PA resembles a Class B amplifier and behaves quite similarly on both power modes. The only difference is the maximum transmit power and current consumption. In addition, the ACLR becomes worse much faster in LPM when the output power increases.

The switch point between the power modes of the PA can be determined based on the measured results. The switching point has 1 dB hysteresis for both directions, which allows smooth transition from HPM to LPM and vice versa. The hysteresis prevents unintentional switching between the power modes when operating near the switching point power level.

Based on the current measurements on the middle frequency channel between the power modes it should be reasonable to stay in LPM up to 7 dBm. As all measured metrics depend on frequency and temperature it is not recommended to decide on the switching point based on single channel results only, thus a margin of several decibels should be considered when selecting the switching point.

6.6. Temperature and Channel Position

The effect of ambient temperature and frequency channel position to the linear performance and gain of the DUT were tested using the measurement setup introduced in Section 5.1. The LTE uplink configuration with eight resource blocks was the same as in Section 5.3. The power amplifier operated in high power mode and applied bias voltage was set to a maximum value of 3.4 V. The output power of the DUT was kept at 23 dBm and the performance was measured with three channels in different ambient temperatures from -15 to 55 degrees. The channels used in the measurements are located on the center and on both edges of the operating bandwidth with frequencies 1852.5 MHz, 1880 MHz and 1907.5 MHz. The resource blocks were located at the channel edges and the worst results were selected.

The linear performance was measured with ACLR according to E-UTRA specifications. The ACLR results of three channels relative to different temperatures are presented in Figure 26.

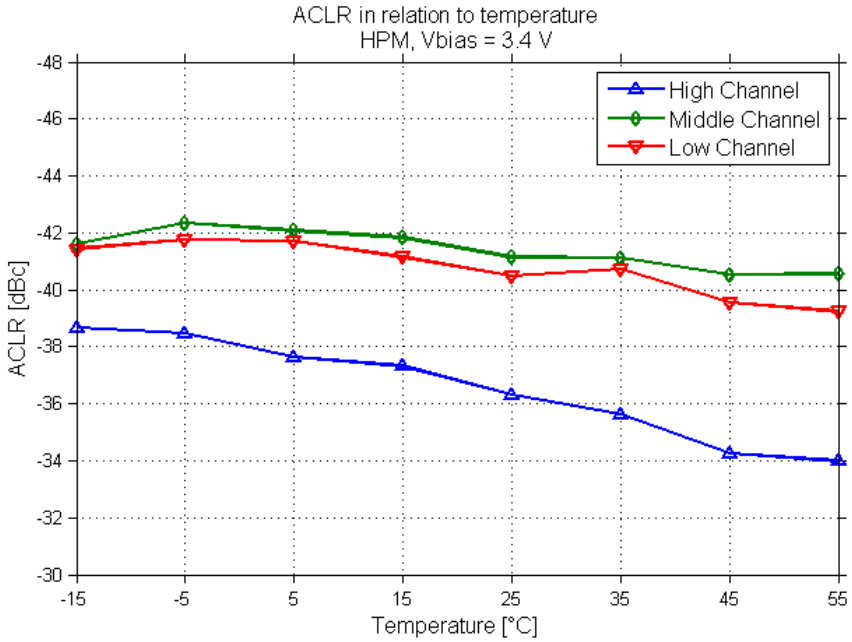

Figure 26. ACLR performance of the DUT in different ambient temperatures.

The ACLR measured on the middle and low channels behaved quite similarly showing only a minor ACLR decrease. The ACLR measured on the high channel was lower on each temperature compared to other channels. The high channel ACLR result of -34 dBc on 55 degrees begins to approach the 3GPP specification limit of -30 dBc.

The considerable difference between channels could be minimized with better impedance matching at higher frequencies of the operating band. The duplex filter causes additional loss on the channels at the edges of the operating band. The pass band of the filter itself has about 1 dB attenuation and on the edges of the pass band it can be nearly 3 dB. To compensate the additional loss at the band edges the input power from the RFIC is increased, which may increase distortion. This fact must be noted when measuring the performance of the DUT on the edge channels of the operating band.

The behavior of total gain of the DUT was also measured with different temperatures and the results are presented in Figure 27. The gain was calculated by subtracting the input power from output power. The figure shows that the gain decreases linearly as a function of temperature. The total gain drop is 2.6 dB on the middle channel and 2.5 dB on high and low channels when the temperature is increased from -15 to 55 degrees. This results in the need for higher input power to reach output power targets.

The gain relation to temperature needs to be compensated. In the final product the temperature compensation is done digitally with a dedicated parameter which increases the input signal power from the RFIC when the gain of the PA decreases so that the output power is kept constant.

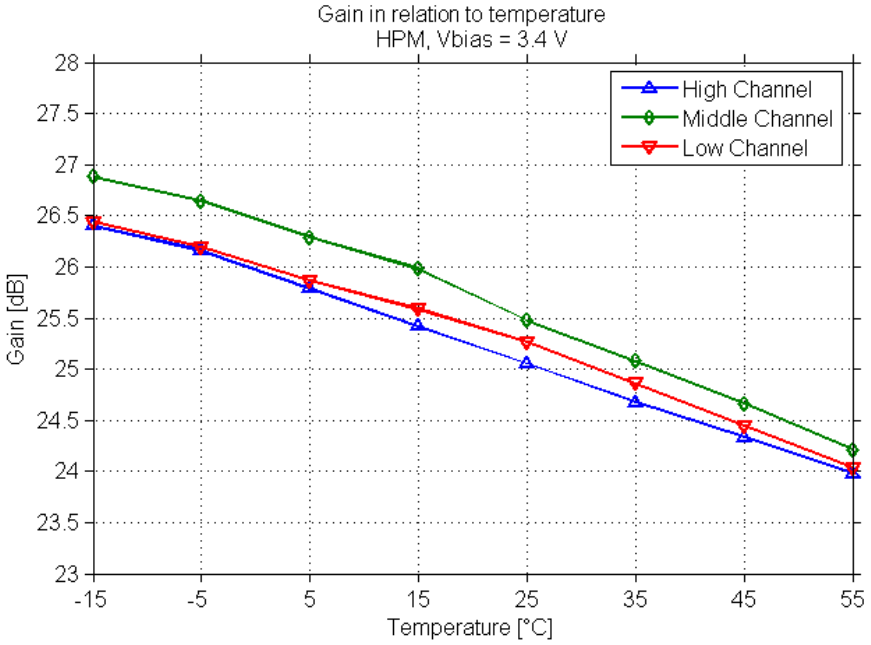

Figure 27. Total gain of the DUT in different ambient temperatures.

6.7. Verification

The suitability of the optimized average power tracking table is verified by applying it to a separate test board. The test board used for verification contains a MMMB PA

supporting average power tracking on LTE and WCDMA. The uplink signal is generated using the RFIC and the bias voltage for the MMMB PA was regulated from the battery voltage using a buck DC-DC converter. The test board has the same RF front-end components from the same manufacturer as in the DUT used for measurements in Section 5.5. Small modifications were made to the impedance matching networks in order to improve overall performance. The performance was measured as conducted from the main antenna port of the mobile device.

The RF tuning of the device and verification measurements are done with Anritsu 8820C Radio Communication Analyzer, which has the option for LTE ACLR measurements with built-in 3GPP E-UTRA and UTRA specific limits. In the tuning phase the RFIC is adjusted so that output powers and other parameters are fulfilling the requirements. The bias voltages for average power tracking are set in the same tuning phase. The DC-DC converter is used to supply voltages to the power amplifier module according to tuned values.

The software used for tuning is provided by the RF chipset manufacturer. The bias voltage adjustment in RF tuning phase uses the APT table as a base and does not follow strictly the bias voltages and output powers from the APT table. Apparently the tuning software sets the voltages a little higher than stated in the APT table as the voltage values are interpolated to the power levels below maximum power level of each power mode. So in HPM the bias voltage on 23 dBm is tuned properly to 3.3 V and on LPM to 2.5 V at 10 dBm according to the APT table, while voltages for intermediate power levels are marginally higher. This is a limitation set by the RF tuning software.

6.7.1. Adjacent Channel Leakage Ratio

Verification measurements were performed with a 5 MHz transmission bandwidth for E-UTRA$_{ACLR}$, UTRA$_{ACLR1}$ and UTRA$_{ACLR2}$, and the corresponding measurement bandwidths and limits are presented in Section 3.2. The rest of the transmission configurations were the same as in Section 5.3. The additional frequencies to the 1880 MHz middle channel were low and high channels with 1852.5 MHz and 1907.5 MHz, respectively. The verification measurements were performed on three channels to ensure that the specified requirements are fulfilled over the whole operating band.

A wide output power sweep from -12 dBm to maximum output power of 23 dBm was performed for the test board including both low power and high power mode output power regions. Because the eight resource blocks used in transmission were allocated on both sides of the transmission bandwidth in separate measurement cases, only ACLR results with RB allocation closer to adjacent channel are taken into account as they result in worse measured ACLR.

Figure 28 shows the ACLR for E-UTRA of the test board used for the verifications. On the figure the middle channel results are marked in green, low channel in red and high channel in blue. The break point in the figure shows the switching point of the PA power modes, which is set to 3 dBm. The PA operates in low power mode up to 2 dBm and starting from 3 dBm the high power mode is turned on. The switch point is set at 3 dBm so that the ACLR remains below -40 dBc on all three channels.

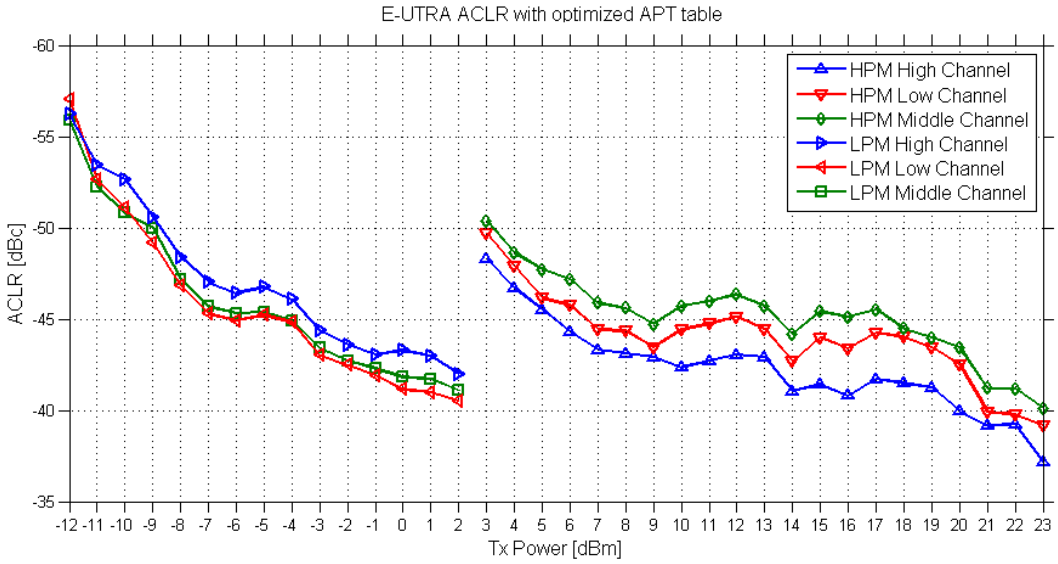

Figure 28. E-UTRA ACLR performance on different TX power levels.

The effect of different ACLR performance on different channels can be seen from Figure 28. In HPM the ACLR on the low and high channel shows worse results when compared to performance on the middle channel. This is because the used APT table was generated using measurement results from the middle channel. The applied bias voltage for 23 dBm was 3.3 V resulting in ACLR = -40 dBc on the middle channel in performance measurements as can be seen in Figure 18. The bias voltage on the maximum power level could be increased to 3.4 V to improve the ACLR performance on the high channel to increase margin to the ACLR limit of the 3GPP specification.

The ACLR performance on the middle and low frequency channels is quite similar on all output power levels, when the PA is operating in LPM. Interesting case is the ACLR behavior in LPM on high frequency channel, where the measured ACLR is several decibels better compared to ACLR on the middle channel.

When the PA operates in high power mode and requested output power is higher, the ACLR on the high channel is notably worse compared to the middle and low channel performance. This can be due to the differences in internal matching between the power modes of the PA module. Also the impedance matching at the output of the power amplifier is optimized on higher and maximum power levels as the linear performance of the PA tends to decrease the most on those power levels.

Figure 29 presents the ACLR performance measured with UTRA channel limits. The measured ACLR results between E-UTRA and UTRA seem to have a 5 dB difference in favor of UTRA while the form of the graphs remains quite similar. The adjacent channel measurement bandwidths for E-UTRA and UTRA are presented in Table 3 and Table 4, respectively. Basically the difference between measured E-UTRA$_{ACLR}$ and UTRA$_{ACLR1}$ is the used measurement bandwidth, which is narrower with the UTRA$_{ACLR1}$ measurement. This causes a better ACLR as the integrated power on adjacent channel is measured using a narrower bandwidth.

In both E-UTRA and UTRA ACLR measurements the HPM performance was the best on the middle frequency channel and the worst measured ACLR performance was on channels located on both sides of the band with resource blocks allocated near the edge of the transmission bandwidth. One reason for this behavior is the band specific

filter component after the power amplifier. The filter begins to attenuate the signal when the channel used in transmission is located at the edge of the pass band of the filter.

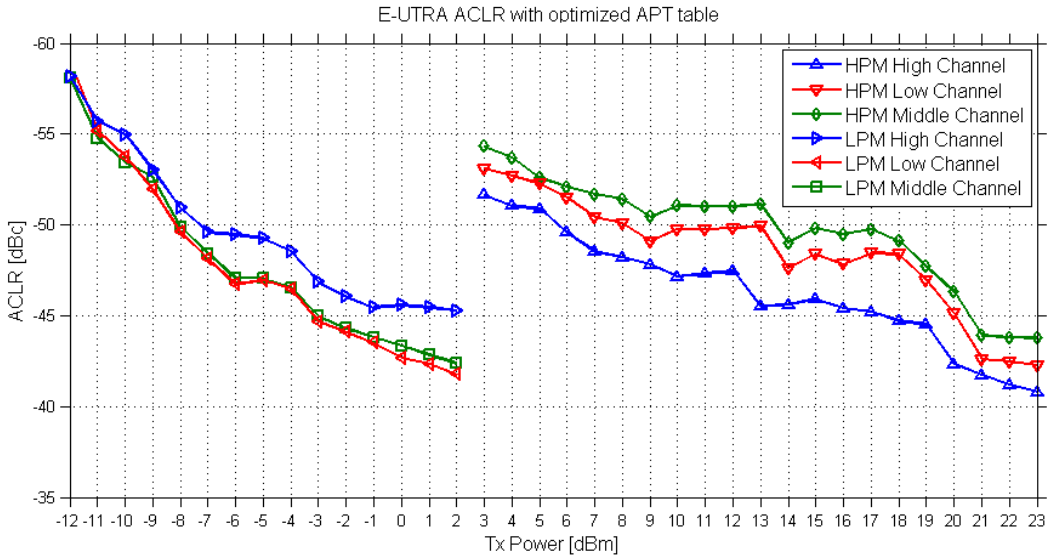

Figure 29. First UTRA channel ACLR on different TX power levels

The second adjacent channel leakage ratio measurement results of $UTRA_{ACLR2}$ were all below -55 dBc, which is not near the 3GPP specification limit of -36 dBc or even the -40 dBc limit used in this thesis. It seemed that $UTRA_{ACLR2}$ results were not affected by the PA bias voltage variation, therefore $UTRA_{ACLR2}$ results are not observed.

Due to the limited capabilities of the RF tuning software the bias voltages were tuned higher than stated in the applied APT table. This causes the ACLR verification results to differ from the measured results of the DUT. Figure 18 shows how the ACLR improves greatly when the applied bias voltage is marginally increased. As an example, the measured ACLR is improved by 5 dB with a 300 mV bias voltage increase at 17 dBm output power level. This is acceptable as the linear performance of the power amplifier improves with higher bias voltages and a sufficient margin is needed for the final product due to component variations and behavior. While the 3GPP performance requirements are fulfilled the downside is degraded efficiency.

There are several reasons why the measured results of the DUT and verification measurements of the test board are different. For example, the LTE signal generated with the signal generator with additional losses from RF cables is not as distortion free compared to the RFIC generated signal. Also the mobile device used for verification measurements has the latest and optimized impedance matching networks which improve linearity.

6.7.2. Spectrum Emission Mask

Finally the spectrum emission mask of the mobile device with the generated APT table was measured. Figure 30 shows the 3GPP spectrum emission mask limits of the 5 MHz transmission bandwidth for different offset frequencies from Table 2. The SEM was measured for three channels and used frequency offsets from the operation band edges

with corresponding measurement resolution bandwidths are presented in Table 8. The output power was set to maximum 23 dBm and the applied bias voltage was set to 3.3 V according to the generated APT table. All three channels were measured with ten different frequency offsets.

Table 8. Frequencies and resolution bandwidths used in spectrum emission mask measurements

Frequency offset	**Resolution Bandwidth**
±0.015 MHz	30 kHz
±1.5 MHz	1 MHz
±5.5 MHz	1 MHz
±6.5 MHz	1 MHz
±9.5 MHz	1 MHz

The measured power on the high channel seems to be a little higher when compared to the other channels when measured near the operating band. The results further out results show minor differences between the frequency channels. The verification measurement results on all three channels clearly fulfill the 3GPP specified limits for the spectrum emission mask.

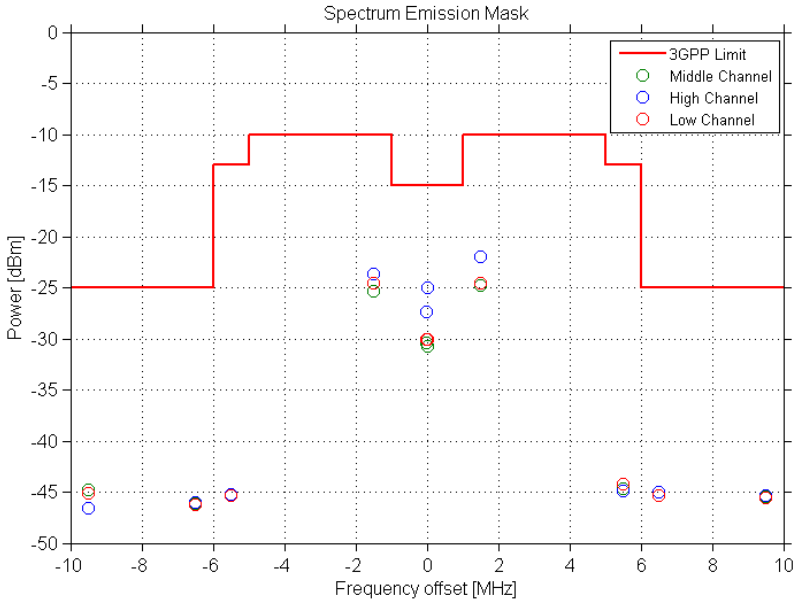

Figure 30. Spectrum emission mask verification measurement.

The verification measurements made with the test board show that the average power tracking with tuned bias voltages generated from the measured results with the optimization algorithm fulfill the 3GPP ACLR and SEM specifications.

7. DISCUSSION

The measurement system presented in this thesis seems adequate and well suited for the purpose. It can be used to generate the average power tracking table with optimized bias voltages for the power amplifier in a mobile device. The algorithm for the measurement setup is used to measure the performance of the DUT with one parameter, which in this case is the bias voltage. As the most of the commercial power amplifier modules support also the quiescent current parameter, the next iteration of the algorithm should include both parameters. This could be implemented by selecting various proper quiescent current values for various power modes and performing the bias voltage optimization algorithm presented in Section 5.3 for the power amplifier with selected quiescent current values.

At its current stage the algorithm to generate the APT table for the power amplifier uses the measured adjacent channel leakage ratio to ensure sufficient linearity across the output power range. The algorithm supports multiple channel and temperature measurement sequences and generates the APT table according to the worst measured non-linear performance. This could be improved by adding the measured current consumption parameter to the result selection phase so that the minimum voltage with the minimum current consumption to reach the set ACLR target is saved for the APT table. In this way the voltages are optimized better in terms of efficiency instead of linearity performance alone. Also forming the APT table the ACLR target of -40 dBc used in this thesis has 10 dB margin to the 3GPP E-UTRA requirements. This is quite large margin and it is more suitable for High-Speed Packet Access (HSPA) used in 3G transmission due to its more complex modulation scheme. For E-UTRA ACLR a target value with smaller margin could be considered.

The time to measure one power amplifier depends strongly on the output power range and the resolution of the bias voltage adjustment. In its current state, it takes approximately eight hours to measure one power amplifier module with the parameters used in this thesis presented in Table 7. The measurement pace could be increased by performing a binary search to find the output power targets instead of linear increase of input power. The binary search is already used in the fine tune phase of the measurement procedure.

As stated in Section 5.1, the setup and the DUT uses a standard 50 ohm matching for input and output, and the APT table obtained with the measurement results is valid only for the case of 50 ohm impedance. In a handheld mobile device the impedance of the antenna changes depending on circumstances, thus transmit signal power delivered to the load varies. The effect of impedance variance can be observed with load-pull measurements. In load-pull measurements the linear performance of the DUT is measured in various output impedance mismatch cases, and the load-pull results would be informative addition to the results from the measurement setup when analyzing the voltage selection. Unfortunately it was not possible to perform load-pull measurements for the DUT for this thesis.

To achieve full benefit from the generated APT table a more precise RF tuning system is needed. The software used for RF tuning uses the applied APT table more as a guideline than a rule and does not set the PA bias voltages accurately according to the APT table. While the output of the DC-DC converter can be adjusted accurately, the current tuning system wastes the full potential of the optimized APT table due to the limited support of parameter configuration.

8. CONCLUSION

The purpose of this thesis was to implement a setup for measuring the performance of an LTE RF power amplifier under different bias voltage and output power configurations. Designing of an algorithm for processing the results was also part of this thesis. The algorithm was used for the measurement results so that the average power tracking efficiency improvement technique could be applied with the maximum efficiency while maintaining the linear performance of the device.

Most of the performance measurements were performed on the middle frequency channel of operating band 2 at 25 °C ambient temperature for both low and high power modes of the PA. The measurements were done with a dedicated measurement setup, which consist of a signal generator, a power meter and a spectrum analyzer. The measurements were performed on a DUT that includes all the main RF front-end components for a transmitter chain, such as the PA, duplex filters and an antenna switch.

The measured performance metrics were ACLR, gain, PAE and current consumption. Measurement results of both power modes showed that all above-mentioned metrics had a relation to the applied bias voltage and output power level. The ACLR and total gain of the DUT were improved when the bias voltage was increased. To avoid distortion, a higher bias voltage was required to be applied to the power amplifier when the output power level was increased. Current consumption did not seem to be affected by applied voltage; instead the output power was the most affecting factor. The power added efficiency of the DUT is significantly improved with APT compared to fixed voltage.

The effect of the ambient temperature and frequency channel position was also studied in the maximum output power case. The results show that the gain of the DUT decreased while the temperature was increased. The channel position varied the ACLR results so that on channels near the edges of the operating band the linearity decreased compared to the center frequency of the operating band.

The APT table was then generated with a dedicated VBA macro, based on the ACLR performance so that the linear performance requirements were fulfilled with a minimum applied bias voltage. The set ACLR limit in this thesis was -40 dBc. The generated APT table was then verified by applying it to a separate test board with the same front-end components. Differences in linearity performance between the frequency channels became evident and the reasons were discussed. Nevertheless the 3GPP specified minimum requirements for ACLR were fulfilled on every measured frequency channel with an output power region from -12 dBm to 23 dBm. In addition, the emissions located further on the frequency domain were measured in terms of spectrum emission mask. The performance measurement results fulfilled the given 3GPP SEM requirements on three different channels at 23 dBm output power.

9. REFERENCES

[1] Sesia S., Toufik I. & Baker M. (2011) LTE - The UMTS Long Term Evolution: From Theory to Practice, Second Edition. John Wiley & Sons Ltd, Chichester, United Kingdom, 752 p.

[2] Cripps S. (1999) RF Power Amplifiers for Wireless Communications. Artech House, Nordwood, MA, 337 p.

[3] Bumman K., Jinsung C., Daehyun K. & Dongsu K. (2009) Envelope Tracking Technique for Multimode PA Operation. European Microwave Conference, IEEE pp. 429-432.

[4] Cheng N. & Young J.P. (2011) Challenges and Requirements of Multimode Multiband Power Amplifiers for Mobile Applications. Compound Semiconductor Integrated Circuit Symposium (CSICS), IEEE

[5] 3GPP (2013) TS 36.101, Evolved Universal Terrestrial Radio Access; User Equipment Radio Transmission and Reception. September 2013, Version 9.17.0

[6] Raghavan A., Srirattana N. & Laskar J. (2008) Modeling and Design Techniques for RF Power Amplifiers John Wiley & Sons Ltd, Chichester, United Kingdom, 752 p.

[7] Kazimierczuk M. (2008) RF Power Amplifiers. John Wiley & Sons Ltd, Chichester, United Kingdom, 405 p.Whitaker J. (2002) The RF Transmission Systems Handbook. CRC Press LLC, Boca Raton, Florida, 466 p.

[8] Whitaker J. (2002) The RF Transmission Systems Handbook. CRC Press LLC, Boca Raton, Florida, 466 p.

[9] Gillenwater T. & Schindler M. (2013) Technology Trends in Mobile Handsets. Wireless Symposium (IWS), IEEE International

[10] Holma H. & Toskala A. (2009) LTE for UMTS-OFDMA and SC-FDMA Based Radio Access. John Wiley & Sons Ltd, Chichester, United Kingdom, 431 p.

[11] Myung H., Lim J. & Goodman D. (2006) Peak-to-Average Power Ratio of Single-Carrier FDMA Signals with Pulse Shaping. Personal, International Symposium on Indoor and Mobile Radio Communications, IEEE

[12] Rana M.M. (2010) Peak to Average Power Ratio Analysis for LTE Systems. Second International Conference on Communication Software and Networks, IEEE

[13] Gebner C. (2011) Long Term Evolution: A concise introduction to LTE and its measurement requirements. Rohde & Schwarz, Munchen, Germany, 216 p.

[14] Walsh K. & Johnson J. (2009) 3G/4G Multimode Cellular Front End Challenges Part 3: Impact on Power Amplifier Design. RFMD White Paper

[15] Hau G. & Singh M. (2010) Multi-Mode WCDMA Power Amplifier Module with Improved Low-Power Efficiency using Stage-Bypass. Radio Frequency Integrated Circuits Symposium, IEEE, pp. 163 – 166.

[16] MIPI Alliance (accessed 20 January 2014), RF Front End Specification. URL: http://www.mipi.org/specifications/rf-front-end